I

PREPARATION AND DESCRIPTION OF SOME DERIVATIVES OF MOLYBDENUM DICHLORIDE

II

STRUCTURE DETERMINATION OF COMPLEX MOLECULES OR IONS BY X-RAY DIFFRACTION BY SOLUTIONS

Thesis by

Philip Alfred Vaughan

In Partial Fulfillment of the Requirements

For the Degree of

Doctor of Philosophy

California Institute of Technology

Pasadena, California

1949

ACKNOWLEDGMENTS

I wish to express my gratitude to Professor Linus Pauling for suggesting the problems presented in this Thesis and for continued interest in the progress of their solution. I also thank Professor J. H. Sturdivant for his valuable assistance in all phases of this work. His experience in the design of X-ray equipment made possible the rapid and successful construction of a suitable apparatus for producing diffraction photographs of solutions. I wish to thank Professor Verner Schomaker for helpful discussions concerning the preparation and interpretation of the visual intensity curves, and Professor Herbert S. Harned for giving the Chemistry Department a quantity of the chlorocolumbium compound, the structure of which is discussed in this Thesis. Lastly, I am grateful to my wife for her encouragement in my work and her help in preparing this manuscript.

ABSTRACT

I. Preparation and Description of Some Derivatives of Molybdenum Dichloride

The compounds $H_2[Mo_6Cl_8]Cl_6 \cdot 8H_2O$, $(NH_4)_2[Mo_6Cl_8]Cl_2 \cdot H_2O$, and $K_2[Mo_6Cl_8]Cl_2 \cdot H_2O$ have been prepared and analyzed. The space group and unit cell dimensions of the first two compounds have been determined from X-ray diffraction photographs; the axial ratios were also obtained by goniometric measurements. The crystallographic data are

	$(NH_4)_2[Mo_6Cl_8]Cl_6 \cdot H_2O$	$H_2[Mo_6Cl_8]Cl_6 \cdot 8H_2O$
Possible Space Groups	C_{2h}^6 - C 2/c C_s^4 - Cc (probable)	C_{2h}^6 - 2/c C_s^4 - Cc
a_1	19.33 Å	17.30 Å
a_2	14.93 Å	9.12 Å
a_3	9.16 Å	18.63 Å
β	115.2°	98.1°
Unit Cell Volume	2390 Å^3	2910 Å^3
Density of Compound	3.093 gm/cc	-
Molecules per Unit Cell	4	4

II. Structure Determination of Complex Molecules or Ions by X-Ray Diffraction by Solutions

The first part of this section is devoted to a brief theoretical discussion of the application of the visual estimation method to the determination of the structure of a complex compound by X-ray diffraction by its solution. A description of the experimental technique used to obtain suitable photographs

is then presented. It is shown that the method gives satisfactory results for the $PtCl_6^{--}$ and $PtBr_6^{--}$ ions, the structures of which are well known. The structures of the (Cb_6Cl_{12}), (Ta_6Br_{12}), and (Ta_6Cl_{12}) groups were determined by X-ray diffraction by ethanol solutions of $Cb_6Cl_{14}\cdot 7H_2O$, $Ta_6Br_{14}\cdot 7H_2O$, and $Ta_6Cl_{14}\cdot 7H_2O$. It is shown that the diffraction data are consistent with the assumption of a (M_6X_{12}) group in which the metal atoms are at the corners of a regular octahedron and the halogen atoms on the perpendicular bisectors of the edges of this octahedron. The shortest interatomic distances in the (M_6X_{12}) group are

Compound	M - M, Å	M - X, Å	X - X, Å
$Cb_6Cl_{14}\cdot 7H_2O$	2.85	2.41	3.37
$Ta_6Br_{14}\cdot 7H_2O$	2.92	2.62	3.64
$Ta_6Cl_{14}\cdot 7H_2O$	2.88	2.44	3.41

These results are in reasonable agreement with Pauling's theory of intermetallic distances in metals.

TABLE OF CONTENTS

I

PREPARATION AND DESCRIPTION OF SOME DERIVATIVES OF MOLYBDENUM DICHLORIDE

A. Preparation of Molybdenum Dichloride and Some of its Derivatives

In most of the literature on the subject the formulae for divalent molybdenum compounds are represented as derivatives of $(Mo_3X_4)\ X_2$ (molybdenum dihalide), since it has been shown that only one third of the halogen atoms can readily be replaced by other atoms or groups. Recently, Cyrill Brosset has demonstrated that the grouping (Mo_6Cl_8) is present in two derivatives of molybdenum dichloride (1, 2). Therefore, since this grouping is probably present in all divalent molybdenum compounds, formulae of all such complex compounds will be written as derivatives of $(Mo_6X_8)\ X_4$ in this report.

Lindner and coworkers (3,4,5) have investigated the preparation of divalent molybdenum compounds. Of the various methods that have been used for the preparation of molybdenum dichloride, they recommend chlorination of molybdenum metal with phosgene at temperatures of 600 to 620° C. This is the method that has been used throughout this investigation. About 2-4 grams of metal was put into porcelain boats which were placed in a silica combustion tube heated by an electric furnace. Nitrogen was passed through the tube until the correct temperature was reached, and then phosgene was passed through at a rate roughly determined by a small bubbler. At the completion of the reaction the phosgene was shut off, the tube flushed out with nitrogen, and the apparatus allowed to cool. The dichloride was usually extracted from the material remaining in the boats with 30-50 ml of an anhydrous alcohol-ether mixture (5-50 percent alcohol) or

with concentrated hydrochloric acid. The extract was then evaporated and the product washed with dilute nitric acid and water to give a partially hydrolyzed product of variable composition which was soluble in hydrochloric acid. The yields were always small, usually being 3 to 7 percent of the theoretical. Lindner, Haller, and Helwig (4) recommend using temperatures of 600-620°C; however, I observed no significant difference in yield between 550 and 650°C. For the best results I found that the phosgene should be passed through at the rate of about 50 to 100 ml per minute for ten to fifteen minutes. The principal side products are higher chlorides. The pentachloride, being volatile, collects at the cool end of the tube; the trichloride, a dark red powder, is usually present in the boats along with dichloride and unreacted molybdenum. It is, however, practically insoluble in water, acids, and organic solvents.

The following three hydrated derivatives of molybdenum dichloride have been prepared and analyzed:*

(1) Compound obtained by cooling a hot solution of dichloride in concentrated hydrochloric acid.

(2) Compound crystallized from a dichloride solution in approximately 8 percent aqueous ammonium chloride acidified with hydrochloric acid.

(3) Compound obtained by cooling a hot solution of

---

*I analyzed for chlorine by the gravimetric silver chloride method. The molybdenum was titrated with standard potassium permanganate solution after reduction to Mo^{+++} in a Jones reductor (6). In all cases, complete destruction of the complex was assured by oxidation with nitric acid or hydrogen peroxide.

dichloride in approximately 8 percent potassium chloride solution acidified with hydrochloric acid.

The following analytical data were obtained:

	% Mo	% Cl
HCl compound	47.14	41.09
Calculated for $H_2[Mo_6Cl_8]Cl_6 \cdot 8H_2O$ . .	47.25	40.75
NH_4Cl compound	50.2	44.3
Calculated for $(NH_4)_2[Mo_6Cl_8]Cl_6 \cdot 2H_2O$.	50.4	43.5
Calculated for $(NH_4)_2[Mo_6Cl_8]Cl_6 \cdot H_2O$.	51.1	44.1
KCl compound	49.1	42.4
Calculated for $K_2[Mo_6Cl_8]Cl_6 \cdot 2H_2O$. . .	48.5	41.9
Calculated for $K_2[Mo_6Cl_8]Cl_6 \cdot H_2O$ . . .	49.3	42.5

Several investigators have given the above formula for the compound with hydrochloric acid, and there is little doubt that it is the correct one. The monohydrate seems to fit the analytical data for the potassium chloride compound. There is a discrepancy in the case of the ammonium chloride compound; however, it will be shown that the monohydrated compound gives a better unit cell interpretation. For this reason I shall use the formula $(NH_4)_2[Mo_6Cl_8]Cl_6 \cdot H_2O$, although there is still uncertainty. Other investigators report the formation of different hydrates; for example, Lindner, Haller, and Helwig (4) give the formulae $K_2[Mo_6Cl_8]Cl_6 \cdot 6H_2O$ and $(NH_4)_2[Mo_6Cl_8]Cl_6 \cdot 3H_2O$ for compounds formed under conditions somewhat different from those given above.

B. <u>The Crystallography of $(NH_4)_2[Mo_6Cl_8]Cl_6 \cdot H_2O$</u>

This compound crystallizes from acidic ammonium chloride solutions in fairly long, flat yellow crystals which are stable

at room temperature for at least several months. A Laue photograph taken with the X-ray beam parallel to the needle axis showed the presence of a mirror plane parallel to this axis. This indicates a Laue symmetry of C_{2h}. Using MoKα radiation with a zirconium filter, a rotation photograph was made about the needle axis a_3. From this and a gnomonic projection made from the Laue photograph it was possible to calculate the unit cell parameters and deduce the space lattice. The cell parameters are

$$a_1 = 19.57\ \text{Å}$$
$$a_2 \text{ (two-fold axis)} = 15.06\ \text{Å}$$
$$a_3 \text{ (needle axis)} = 9.13\ \text{Å}$$
$$\beta = 115.1^\circ$$

The gnomonic projection was indexed in a satisfactory manner with reflections occurring only from planes with h + k even. This indicates a side centered lattice. The radii of limiting circles were calculated with these parameters, and it was observed that no spots of the corresponding order on the gnomonic projection fell outside of these circles.

Laue photographs were taken along each of the principal axes, and by measuring the angle between zones on the Laue apparatus, angle β was found to be 115.3°. A partial gnomonic projection was made from a Laue photograph taken with the beam parallel to the two-fold axis a_2. Angle measurements on this projection give a value of 115.1° for the angle β.

To obtain better values for the unit cell edges, rotation photographs were taken about a_1 and a_2, and layer line

measurements were made. The final unit cell parameters are given below:

$$a_1 = 19.33\ \text{Å}$$
$$a_2 = 14.93\ \text{Å}$$
$$a_3 = 9.16\ \text{Å}$$
$$\beta = 115.2^\circ$$

Volume of unit cell = 2390 Å^3

The angle β given above is the average of the angles determined by the three methods which have been described.

The density of the substance was found by flotation in a mixture of bromoform and methylene iodide to be 3.093 gm/cc at approximately 23°C. From this and the unit cell volume, the following data were calculated:

Compound	Molecules per unit cell
$(NH_4)_2\{Mo_6Cl_8\}Cl_6 \cdot 2H_2O$	3.90
$(NH_4)_2\{Mo_6Cl_8\}Cl_6 \cdot H_2O$	3.96
$(NH_4)_2\{Mo_6Cl_8\}Cl_6$	4.03

Although the anhydrous compound would give a slightly better value than the monohydrated compound for the number of molecules per unit cell, the difference is not significant, and it has been observed that some water is given off when the compound is heated. Since the latter formula also seems to fit the analytical data better, it is the more probable one.

Goniometric measurements have been made of a crystal mounted with the needle axis vertical. Figure 1 shows the appearance of the crystal with the location of the crystallographic axes. The following measurements were made and the faces indexed:

$(\bar{1}00):(110) = 130^{\circ}47'$
$(110):(100) = 49^{\circ}13'$
$(100):(1\bar{1}0) = 48^{\circ}24'$
$(1\bar{1}0):(\bar{1}\bar{1}0) = 82^{\circ}17'$
$(\bar{1}\bar{1}0):(100) = 49^{\circ}19'$
$(\bar{1}11) = 85^{\circ}15'$ azimuth from face $(\bar{1}00)$; $58^{\circ}25'$ altitude

If a value of 115.2° for the angle β is assumed, the axial ratios are $a_1 : a_2 : a_3 = 1.301 : 1 : 0.613$. This compares with 1.294 : 1 : 0.613 calculated from the rotation photographs.

A Weissenberg photograph was made of the equatorial net perpendicular to a_2, using CuKα radiation. This and the Laue photographs were used to determine the space group. The following observations were made:

(1) No hkℓ reflections with h + k odd occurred in any Laue or Weissenberg photograph. This indicates C-centering.

(2) No h0l reflections appeared on a Laue photograph taken with the beam parallel to a_3. Also, there were no h0ℓ reflections with ℓ odd appearing on the Weissenberg photograph. This indicates a glide plane parallel to (010) with a glide of $\frac{1}{2}a_3$.

The space groups C_s^4 - Cc and C_{2h}^6 - C 2/c are possible with the above extinctions. Observations of etched figures indicated the absence of a center of symmetry; therefore the space group is probably C_s^4 - Cc.

C. <u>The Crystallography of $H_2[Mo_6Cl_8]Cl_8 \cdot 8H_2O$</u>

This compound as grown from concentrated hydrochloric acid solution forms long, almost square prisms which effloresce

slowly. It was necessary to coat crystal specimens with paraffin wax in order to insure their stability. Laue photographs with the X-ray beam parallel and perpendicular to the needle axis show the Laue symmetry to be C_{2h}, the needle axis being the two-fold axis. Zirconium filtered MoKα radiation was used to make a rotation photograph about the two-fold axis, from which it was determined by layer line measurements that $a_2 = 9.12$ Å. The other unit cell parameters were then determined from a gnomonic projection made from a Laue photograph which was taken with the X-ray beam parallel to a_2. The unit cell parameters determined in this manner were

$$a_1 = 17.30 \text{ Å} \quad (b_1 = 0.0584 \text{ Å}^{-1})$$
$$a_2 = 9.12 \text{ Å} \quad (b_2 = 0.1097 \text{ Å}^{-1})$$
$$a_3 = 18.63 \text{ Å} \quad (b_3 = 0.0542 \text{ Å}^{-1})$$
$$\beta = 98.1^\circ$$
$$\text{Volume of unit cell} = 2910 \text{ Å}^3$$

The radii of limiting circles were calculated with these parameters, and it was observed that no spots of the corresponding order on the gnomonic projection fell outside of these circles. The reflections hlℓ with h even were absent in the gnomonic projection, indicating a C-centered lattice. By measuring the layer lines on a rotation photograph taken about a_1, this parameter was determined to be 17.33 Å, checking closely with the above result. The density of this compound has not yet been determined, hence the number of molecules per unit cell is not known with certainty. However, because of the similarity of this compound

with $(NH_4)_2[Mo_6Cl_8]Cl_6 \cdot H_2O$ (space group C_s^4 - Cc, unit cell volume of 2400 Å^3), the most probable number is 4.

Figure 1 gives a sketch of a crystal of $H_2[Mo_6Cl_8]Cl_6 \cdot 8H_2O$. The results of goniometric measurements are

$(100):(00\bar{1}) = 98^\circ\ 5'$
$(00\bar{1}):(\bar{1}00) = 81^\circ 53'$
$(\bar{1}00):(001) = 98^\circ\ 7'$
$(001):(100) = 81^\circ 55'$
$(1\bar{1}\bar{1}) = 46^\circ 21'$ azimuth from face (100); $56^\circ 5'$ altitude
$(\bar{1}\bar{1}1) = 46^\circ 28'$ azimuth from face $(\bar{1}00)$; $56^\circ 6'$ altitude

Angle $\beta = 98.1^\circ$ from these measurements, which agrees with the value determined from the gnomonic projection. From these measurements the axial ratios are $a_1 : a_2 : a_3 = 2.06 : 1 : 1.892$, which compare quite well with the ratios $a_1 : a_2 : a_3 = 2.04 : 1 : 1.900$, determined from X-ray photographs.

In order to determine the space group of this compound, a Weissenberg photograph was made of the equatorial net perpendicular to a_2, using $CuK\alpha$ radiation with a nickel filter. The following observations were made:

(1) No h0 reflection with h odd appeared. This is because of C-centering; hk reflections do not appear with h + k odd.

(2) No h0 with odd appeared. This indicates a glide plane parallel to 010 with a glide of $\frac{1}{2}a_3$.

The space groups C_s^4 - Cc and C_{2h}^6 - C 2/c are possible.

Recently, Cyrill Brosset has worked out the complete structures of $[Mo_6Cl_8](OH)_4 \cdot 14H_2O$ and $[Mo_6Cl_8](Cl_4 \cdot 2H_2O) \cdot 6H_2O$ (2). The grouping $[Mo_6Cl_8]$ was found in which the chlorine atoms are

at the corners of a cube with the molybdenum atoms at the centers of the faces (possibly slightly out of the planes of the faces). Since this basic grouping is undoubtedly present in $(NH_4)_2[Mo_6Cl_8]Cl_6 \cdot H_2O$ and $H_2[Mo_6Cl_8]Cl_6 \cdot 8H_2O$, this investigation was discontinued.

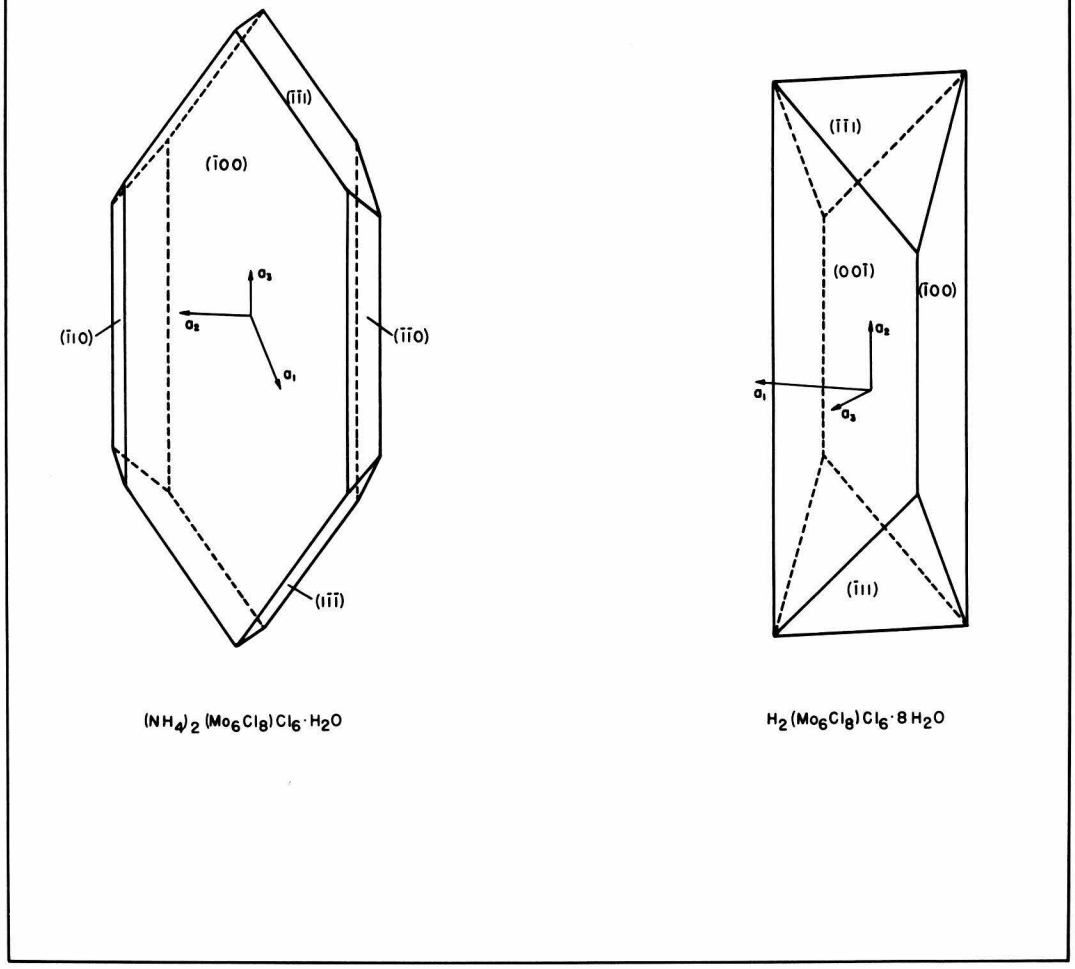

Figure 1

Typical Crystals of $(NH_4)_2[Mo_6Cl_8]Cl_6 \cdot H_2O$ and $H_2[Mo_6Cl_8]Cl_6 \cdot 8H_2O$

II

STRUCTURE DETERMINATION OF COMPLEX MOLECULES OR IONS BY X-RAY DIFFRACTION BY SOLUTIONS

A. Theoretical Discussion

1. Comparison of Calculated and Observed Intensity Functions

The intensity of monochromatic X-rays scattered coherently by any macroscopically isotropic system of atoms can be represented as a function of the scattering angle,

$$I(\varphi) = I_e \sum_i \sum_j f_i f_j \int_0^\infty \rho_{ij}(r) \frac{\sin sr}{sr} dr \qquad 1$$

where

$$I_e = I_0 \frac{e^2}{m^2 c^4 R^2} \frac{1+\cos^2\varphi}{2}$$

and

$$s = \frac{4\pi \sin\frac{\varphi}{2}}{\lambda}$$

The primary beam is assumed to be unpolarized. The summations are over every atom in the system, and each term, therefore, relates to an atom pair (i,j) whose scattering amplitudes are f_i and f_j.* The function $\rho_{ij}(r)$ is the probability that the atoms i and j have the separation r; it is normalized by the condition

$$\int_0^\infty \rho_{ij}(r)\, dr = 1$$

This equation applies to all gases, liquids, amorphous solids, and finely divided crystalline solids consisting of any number of chemical species.

In many cases the integrals in Equation 1 can be evaluated and the equation reduced to the form

---

*A collection of terms is made in all real systems, in which each term occurs a large number of times.

$$I(\varphi) = I_e \sum_i \sum_j f_i f_j T_{ij}(s) \frac{\sin r_{ij} s}{r_{ij} s} \qquad 2$$

where r_{ij} is the average separation of atoms i and j, and T_{ij} depends on the function $\rho_{ij}(r)$. The factor T_{ij} is equal to unity when i = j or when the separation of i and j is a constant.

In the case of gases at low pressure the terms due to intermolecular distances become negligibly small. Equation 1 then assumes a relatively simple form involving only intramolecular distances. This enables one, in most simple cases, to find these distances and hence to determine the molecular structure from a knowledge of $I(\varphi)$. In practice, however, it is usually much easier to use electron diffraction techniques to determine the structure of gas molecules.

The situation for a liquid is more complex. In general it is not possible to neglect intermolecular terms, and the scattering depends on functions representing the separation and relative orientation probabilities for a pair of molecules as well as on the internal parameters of a single molecule. However, Pirenne (7) has pointed out that in many cases the scattering at fairly large angles is approximated very closely as a function of intramolecular terms only. The scattering function of liquid carbon tetrachloride is an example (8,9). This is true because the $T_{ij}(s)$ functions associated with the longer intermolecular terms decrease quite rapidly as s increases. However, this fact is of little value for molecular structure determination,

since most liquids are volatile and the electron diffraction techniques may readily be applied. Therefore the diffraction pattern of a liquid is generally used to investigate such structural properties as free rotation of molecules and other questions of short range ordering in the liquid state.

In general the problem becomes even more complex in the case of a solution, since the expression for the scattered intensity will then involve terms due to all three types of intermolecular interactions as well as to intramolecular distances in both the solvent and solute. However, if the atoms composing the solute have a much higher atomic number than those of the solvent and have a relatively high concentration, all terms except those due to the interatomic distances in the solute molecules will be relatively small. If smaller terms are neglected, the scattering function will be like that of a gas, having the form

$$I = I_e N \sum_i \sum_j f_i f_j T_{ij} \frac{\sin r_{ij} s}{r_{ij} s} \qquad 3$$

where N is the number of diffracting molecules and the summations are now over every atom in a single molecule of solute. In this Thesis the simplified Equation 3 has been applied in order to investigate the structures of a few complex ions and molecules in solution.

In order to apply the above theory, a method has been used which was developed in these Laboratories for determining the structures of complex molecules by electron diffraction. The

first step, of course, is to obtain suitable photographs, which was done by a technique to be described in the next section of this Thesis. From these photographs a curve is drawn by visual observation and measurements which represents the variation of blackening across the film, but which leaves out the background (nonfluctuating) blackening and the damping; this curve is commonly called the visual curve. This visual curve is to be compared with the reduced intensity function

$$I_c'(s) = \frac{K}{\overline{f_i f_j}} \sum_i \sum_j f_i f_j T_{ij} \frac{\sin r_{ij} s}{r_{ij}} \qquad 4$$

where k is a proportionality constant and $\overline{f_i f_j} = \frac{1}{n(n-1)} \sum_i \sum_j f_i f_j$, $(i \neq j)$, n being the number of atoms in the molecule. If $\frac{f_i f_j}{\overline{f_i f_j}}$ is very nearly independent of s for each term, this equation may be approximated by the simpler expression,

$$I_c'(s) = \sum_i \sum_j A_{ij} T_{ij} \sin r_{ij} s \qquad 5$$

where A_{ij} is independent of s and is an appropriate average of $\frac{k f_i f_j}{r_{ij} \overline{f_i f_j}}$ over the region of observation.

We must now consider the form of the function T_{ij}. For all of the molecules investigated in this Thesis, it will be assumed that the functions $\rho_{ij}(r)$ in Equation 1 can be approximated by exponentials of the form

$$\rho_{ij}(r) = \frac{1}{2\sqrt{\pi a_{ij}}} e^{-\frac{(r-r_{ij})^2}{4a_{ij}}} \quad *$$

In order to evaluate the integral of Equation 1, we make the approximation that

$$\frac{1}{r} e^{\frac{(r-r_{ij})^2}{4a_{ij}}} \sim \frac{1}{4r_{ij}} e^{\frac{(r-r_{ij})^2}{4a_{ij}}}$$

which will be very nearly correct over regions for which $\rho(r)$ is large if $\frac{1}{\sqrt{a}} >> |r - r_{ij}|$. We then find that $T_{ij} = e^{-a_{ij}s^2}$ and Equation 5 becomes

$$I_c'(s) = \sum_i \sum_j A_{ij} e^{-a_{ij}s^2} \sin r_{ij}s \qquad 6$$

The structure determination consists of finding values of the molecular parameters which, when used to calculate a theoretical $I_c'(s)$ from Equation 6, will give the best agreement with the observed $I_o'(s)$. The punched card technique developed in these Laboratories (11) was used to calculate these theoretical curves. In order to apply this technique we must use the intensity equation in the unintegrated form,

$$I_c'(s) = \sum_i \sum_j \frac{A_{ij}}{2\sqrt{\pi a_{ij}}} \int_{-\infty}^{\infty} e^{-\frac{(r-r_{ij})^2}{4a_{ij}}} \sin rs \, dr \qquad 7$$

---

*Since this function is characteristic of temperature vibrations, the constant a_{ij} is called the temperature factor of the distance r_{ij}. This nomenclature will be used even if temperature vibrations are not considered to be responsible for the decline of amplitude with increasing angle. James (10) has discussed the effects of temperature vibrations on X-ray scattering functions.

The integrals in this expression can be closely approximated by sums; the expression is then

$$I_c'(s) = \sum_i \sum_j \left(\sum_{k=-N}^{N} \frac{A_{ij}}{2\sqrt{\pi a_{ij}}} e^{-\frac{(k\delta r)^2}{4a_{ij}}} \sin s(r_{ij} + k\delta r) \right) + \sum_l \sum_m A_{lm} \sin r_{lm} s \qquad 8$$

where δr is an appropriate interval of $|r - r_{ij}|$ and N is chosen so that the amplitude is negligibly small for differences greater than $N\,\delta r$. The second sum is taken over terms for which a_{ij} is zero. This is the form which was used for the calculation of all theoretical curves.

2. The Radial Distribution Method

Although in principle the foregoing discussion provides a method of determining the most probable set of parameters by trial and error, we would like to be able to determine the approximate sizes of these parameters by a more direct method. To do this, it is convenient to apply the radial distribution method which has been widely used in electron diffraction investigations. The radial distribution function (or integral), D(r), used throughout this investigation is defined by the equation

$$D_o(r) = \int_o^{s\,max.} e^{-a's^2} I_o'(s) \sin rs \; ds \qquad 9$$

where $I_o'(s)$ is the observed intensity function. If a', which is often called the artificial temperature factor, is chosen

so that $e^{-a's^2}$ is small for $s = s_{max}$, then this integral will be given to a satisfactory degree of approximation by

$$D(r) = \int_0^\infty e^{-a's^2} I'(s) \sin sr \, ds \qquad 10$$

If we put into this integral the expression for $I_c'(s)$ given by Equation 6 and carry out the integration, the result is

$$D_c(r) = \sum_i \sum_j \frac{A_{ij}}{4} \sqrt{\frac{\pi}{a'+a_{ij}}} \, e^{-\frac{(r-r_{ij})^2}{4(a'+a_{ij})}} + \sum_i \sum_j \frac{A_{ij}}{4} \sqrt{\frac{\pi}{a'+a_{ij}}} \, e^{-\frac{(r+r_{ij})^2}{4(a'+a_{ij})}} \qquad 11$$

All of the terms in the second summation are small for positive values of r and can be neglected. It is seen that D(r) is then a sum of Gaussian curves whose maxima occur at r_{ij}, whose areas are proportional to the amplitudes A_{ij}, and whose half widths are given by $w_{\frac{1}{2}} = 4\sqrt{\ln 2 \times (a' + a_{ij})}$. The radial distribution function can be expected to give valuable information concerning the values of important interatomic distances and their temperature factors. Moreover, the above arguments are independent of our neglect of solvent scattering and intermolecular interactions. Therefore, observations of D(r) may tell us if such neglect is permissible. In practice D(r) is evaluated by approximating the integral in Equation 9 by the sum

$$D_o(r) = \sum_{l=0}^{N} \delta s \, e^{-a' l^2 (\delta s)^2} I'(l \, \delta s) \sin r l \, \delta s \qquad 12$$

where $N_\delta s = s_{max}$. After finding approximate values for the molecular parameters by the application of Equation 12 to the observed intensity curve, a refinement is carried out by means of a suitable trial and error method. It is to be noted that since the units of the amplitudes A_{ij} in Equation 6 are quite arbitrary, the observed peaks in $I'_o(s)$ and in $D_o(r)$ have only relative significance.

B. Description of Apparatus

One of the difficulties encountered in attempting to apply the theory described in the last section is that of obtaining suitable photographs from which an $I'_o(s)$ curve can be drawn. A satisfactory photograph must show enough maxima (or apparent maxima) to make a reasonably unique structure selection possible. It is also desirable that the spacing of these maxima be small enough to provide good contrast. In order to meet these conditions it is necessary to use a comparatively short wave length if the film distance is of the order of 5 cm. Tungsten Kα radiation was used in all of the work described in this Thesis. Since a relatively high voltage is required to excite the tungsten Kα lines, the continuous spectrum is quite strong. This makes it absolutely necessary to use some sort of crystal monochromator in order to obtain a reasonably pure spectrum.

A hot-cathode, tungsten-target tube made by the Lee X-ray Tube Company was the radiation source. In most cases, the exciting voltage was 100 kilovolts peak, a current of approximately 15 milliamperes being used. The current was half-wave rectified

by means of valve tubes. In order to reduce insulating difficulties the target was maintained at +50 and the cathode at -50 kilovolts peak. The target cooling water passed through approximately 100 feet of rubber tubing in order to reduce current loss to a reasonable amount. The high voltage was supplied by a Norelco industrial X-ray transformer.

The camera consisted of a steel plate on which were mounted the monochromator, the pinhole system, two lead shields, and a removable film holder. The monochromator was a galena crystal mounted so that the X-rays could be reflected from a (100) face into a round pinhole. It could be rotated about an axis passing through the reflecting surface to obtain the desired wave length. The pinhole was approximately 0.8 mm in diameter and 3.2 cm long. The diffracting solution, contained in a thin-walled glass capillary tube, was waxed to the face of the pinhole. The flat film holder consisted of two sheets of black celluloid secured to an aluminum frame. The film and intensifying screens were placed in a black paper envelope between these sheets, which were then screwed firmly together. The film holder was attached to a frame which could be moved parallel to the pinhole on three grooved tracks. A lead shield was placed completely around the monochromator with only a small hole directly in back of the galena crystal. This was to prevent any direct or scattered radiation from reaching the film by any path other than the pinhole. It was also possible to adjust this screen to prevent direct radiation from passing through the pinhole. As an additional precaution, a flat sheet of lead with a hole in it

was placed close to the capillary tube, between the solution sample and the film.

The distance from the pinhole face to the front surface of the film holder was measured within ±0.05 mm by means of a simple tripod gage. The remaining distance to the film was just the sum of the thicknesses of the front plastic sheet, the front intensifying screen, and a sheet of black paper. This was measured with a micrometer caliper. The sum of these distances, the distance from the face of the pinhole to the film, was thus accurately determined and was kept constant by means of a spacing bar. To determine the sample-to-film distance for each exposure, it was therefore only necessary to measure the distance from the face of the pinhole to the center of the capillary tube, which was done with a steel scale.

In all the photographs made with this apparatus, Eastman Screen Film was used with Patterson Hi-Speed Intensifying Screens. For most solution photographs, the exposures were of the order of five days.

The apparatus was adjusted by rotating the monochromator crystal until the tungsten $K\alpha$ line was reflected directly through the pinhole. Maximum intensity was then obtained by moving the whole camera with respect to the target. The intensity and appearance of the beam were observed for different monochromator and camera positions by making 30-second exposures on screen film without screens. When the apparatus was in correct adjustment, the beam would produce a spot which was nearly round and had a dark vertical line through its center. The wave

length was measured by taking powder photographs of a sample of galena, the unit cell of which ($a = 5.92$ Å) had been measured previously with standard powder apparatus. Wave length measurements were made three times during the preparation of the solution photographs to be described. The results of these measurements are given in Table 1. In each case the calculated wave length was very close to 0.210 Å, the average wave length of the tungsten $K\alpha$ lines, and this value has been assumed in all calculations.

Examination of these powder photographs also gives one an idea of the resolution obtainable with the apparatus. A schematic diagram of the photograph dated 8/17/48 is given in Figure 2. The heights of the lines are approximately proportional to the intensities relative to other rings in the same neighborhood. For comparison, the calculated diffraction pattern of galena is also given. In this diagram the heights of the lines are proportional to F^2 multiplied by the multiplicity factor and the interplanar spacing. Lines separated by more than 0.4 mm on the film were, in general, resolved.

In all of the photographs obtained with this apparatus the pattern on the right side of the film (as one looks toward the X-ray tube) was much more distinct than that on the left. This phenomenon was so pronounced that all measurements and observations were made on the right side, radii being measured instead of diameters. This is probably caused by an impure spectrum which would have an unsymmetrical effect on the photograph. That this is so can readily be seen by referring to Figure 3.

Table 1

Date of Film		6/16/48			8/17/48			10/9/48		
Camera Distance		5.365 cm			5.24 cm			5.24 cm		
Exposure		720 m.a.h.			730 m.a.h.			735 m.a.h.		
Indices of line	d(average) Å	Radius cm	d*, Å	λ, Å	Radius cm	d*, Å	λ, Å	Radius cm	d*, Å	λ, Å
(111)	3.43	0.32	3.50	0.205	0.31	3.55	0.203	0.321	3.43	0.210
(200)	2.97	0.395	2.94	0.219	0.37	2.98	0.210	0.375	2.93	0.207
(220)	2.10	0.545	2.08	0.212	0.53	2.08	0.210	0.527	2.10	0.210
(311),(222)	1.757	0.65	1.745	0.212	0.63	1.754	0.211	0.626	1.773	0.208
(400)	1.484	-	-	-	0.743	1.494	0.208	-	-	-
(331),(420)	1.337	0.84	1.353	0.208	0.825	1.349	0.208	0.825	1.348	0.209
(422)	1.210	0.94	1.214	0.209	0.925	1.204	0.211	0.906	1.216	0.209
(511),(333)	1.142	1.00	1.123	0.214	0.98	1.139	0.211	0.964	1.145	0.210
(600),(531),(442)	0.995	1.15	0.997	0.210	1.128	0.994	0.210	1.12	0.997	0.210
(620)	0.939	1.24	0.926	0.213	1.193	0.940	0.210	1.194	0.938	0.210
(553),(622)	0.898	1.30	0.887	0.213	1.25	0.899	0.210	1.255	0.898	0.210
(551),(711),(640)	0.827	1.40	0.824	0.211	1.345	0.844	0.206	1.366	0.829	0.210
(642)	0.793	-	-	-	-	-	-	1.425	0.796	0.209
(553),(731)	0.772	-	-	-	-	-	-	1.474	0.770	0.210
(642),(553),(731)	0.783	1.475	0.785	0.209	1.442	0.783	0.210	-	-	-
(733),(820),(644)	0.720	1.61	0.722	0.210	1.565	0.725	0.208	-	-	-
(660),(555),(822) (757),(662)	0.687	1.70	0.687	0.210	1.67	0.684	0.211	-	-	-
Wave Length (average), Å				0.2109			0.2092			0.2094

*Calculated with $\lambda = 0.210$ Å, the wave length of $WK\alpha$.

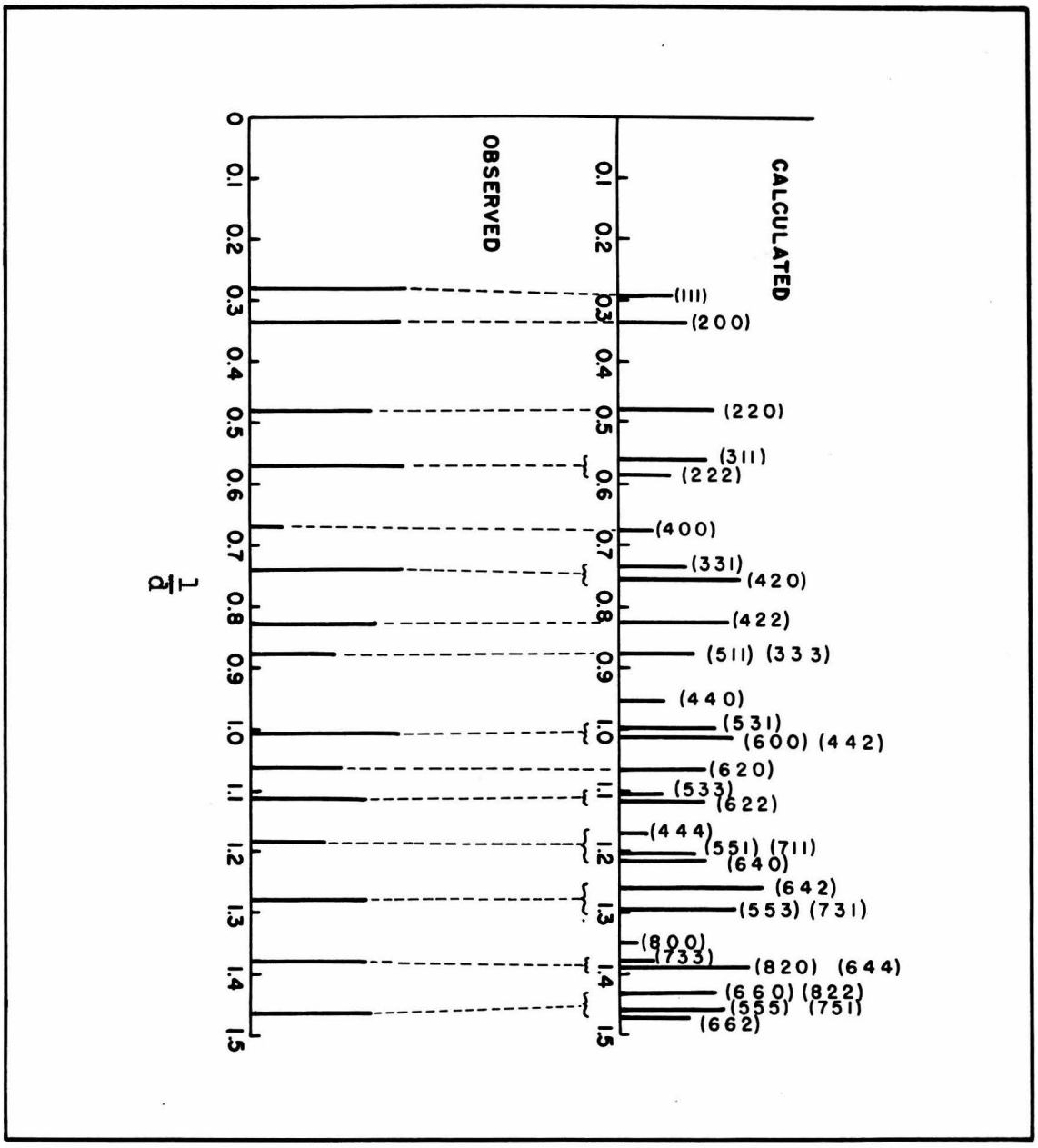

Figure 2

Observed and Calculated Diffraction Patterns

of Galena Powder

Let x be a ray of the proper wave length which leaves the target, is reflected from the monochromator at a Bragg angle θ, and is diffracted by the sample at some angle φ_x. Also, let x' be another ray which leaves the target and is reflected from the monochromator at an angle $\theta + \Delta\theta$. However, $\Delta\theta$ is small enough so that x' can still get through the pinhole. Let ray x' be diffracted by the sample at an angle, $\varphi_{x'}$, such that $\frac{\sin \frac{1}{2}\varphi_{x'}}{\lambda_{x'}} = \frac{\sin \frac{1}{2}\varphi_x}{\lambda_x}$. Now, since its Bragg angle is greater, $\lambda_{x'} = \lambda_x + \Delta\lambda > \lambda_x$, and hence $\varphi_{x'} = \varphi_x + \Delta\varphi > \varphi_x$. Obviously, then, the angle between x and x' will be $\Delta\varphi - \Delta\theta$ on the right side and $\Delta\varphi + \Delta\theta$ on the left side. If L is the perpendicular distance from the sample to the line on which x and x' cross on the right side of the film, and D is the path distance from the target to the sample, it can be shown that

$$L = \frac{D \cos^2 \varphi}{\frac{2 \tan \varphi/2}{\tan \theta} - 1} \qquad \text{(approximately)}$$

It is obvious that x' is parallel to x (since $L = \infty$) after diffraction if $\varphi = 2 \arctan (\frac{1}{2} \tan \theta)$, or, since θ is small, approximately if $\varphi = \theta$. For diffraction angles larger than this, the beam converges. For smaller angles, and particularly for negative angles (corresponding to diffraction on the left side), L is negative and the beam diverges. With the above equation it can be demonstrated that, because of this effect alone, the angular range of φ subtended by the two rays x and

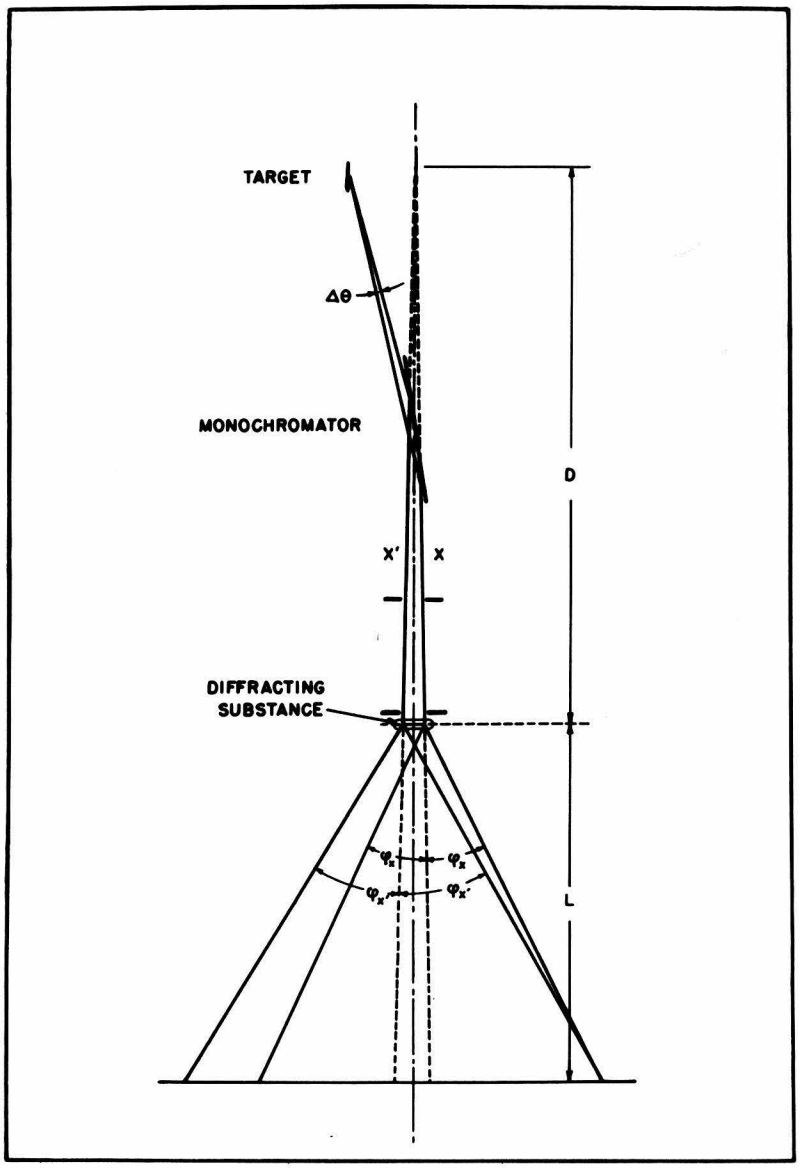

Figure 3

Experimental Arrangement and Illustration

of the Focussing Phenomenon

x' when they strike the film is approximately 1.5° for $\varphi = 20^\circ$. The distance between principal maxima for the compounds considered in this Thesis is from 3 to 5°. The finite size of the focal spot on the X-ray tube target also produces an effect similar to that discussed above, tending to cause the different wave lengths to converge on the right side and diverge on the left side. Experience with the apparatus described in this section indicates that observations made on the film become somewhat unreliable at 20 to 22°, and the limit of observation is approximately 26° ($q = 75$). The above phenomena are probably the biggest factors causing decrease of resolution, and to a large extent they determine how far out on the film useful information can be observed.

C. Trial Experiments with Compounds of Known Structure

1. Bromoplatinic Acid

In order to give the method outlined in the first two sections a satisfactory trial, a solution photograph of bromoplatinic acid was made, the structure of this compound being well known. A saturated aqueous solution was used. The visual curve is given in Figure 4 and the positions of the maxima and minima in Table 2. The maximum labeled 1 is the first maximum that can be seen on the photograph but is the second maximum on the visual curve of Figure 4. The first maximum on the visual curve cannot be seen on the film; indeed it is not actually present in the unsimplified intensity function since $\frac{\sin sr}{sr}$ does not go to zero as s approaches zero. However, since we do not include the

1/s factor in the function $I'_c(s)$ as given by Equation 6, this

Table 2

Feature max	Feature min	q_{obs}	q_{calc} T.F. = 0.010	$\frac{q_{calc}}{q_{obs}}$
1		14.2	16.5	(1.162)
	1	16.8	18.5	(1.102)
2		19.9	21.0	(1.056)
	2	27.0	26.5	(0.981)
3		32.6	32.5	0.997
	3	39.5	39.2	0.992
4		45.7	45.7	1.002
	4	54.3	54.6	1.006
5		61.6	61.4	0.997
	5	69.3	68.5	(0.988)
6		76.2	75.2	(0.987)
		Average (5 features)		0.999

expression does go to zero. The first maximum is included so that the radial distribution integration can be made with zero as the lower limit. It was placed at a distance from the origin of approximately one quarter of the average distance between principal maxima.

The radial distribution integral was calculated by means of the punched card technique developed in these Laboratories for electron diffraction calculations (11). A transformation was made to the variable q, where $q = \frac{70}{4\pi}s = \frac{70}{\lambda}\sin\frac{\phi}{2}$. The

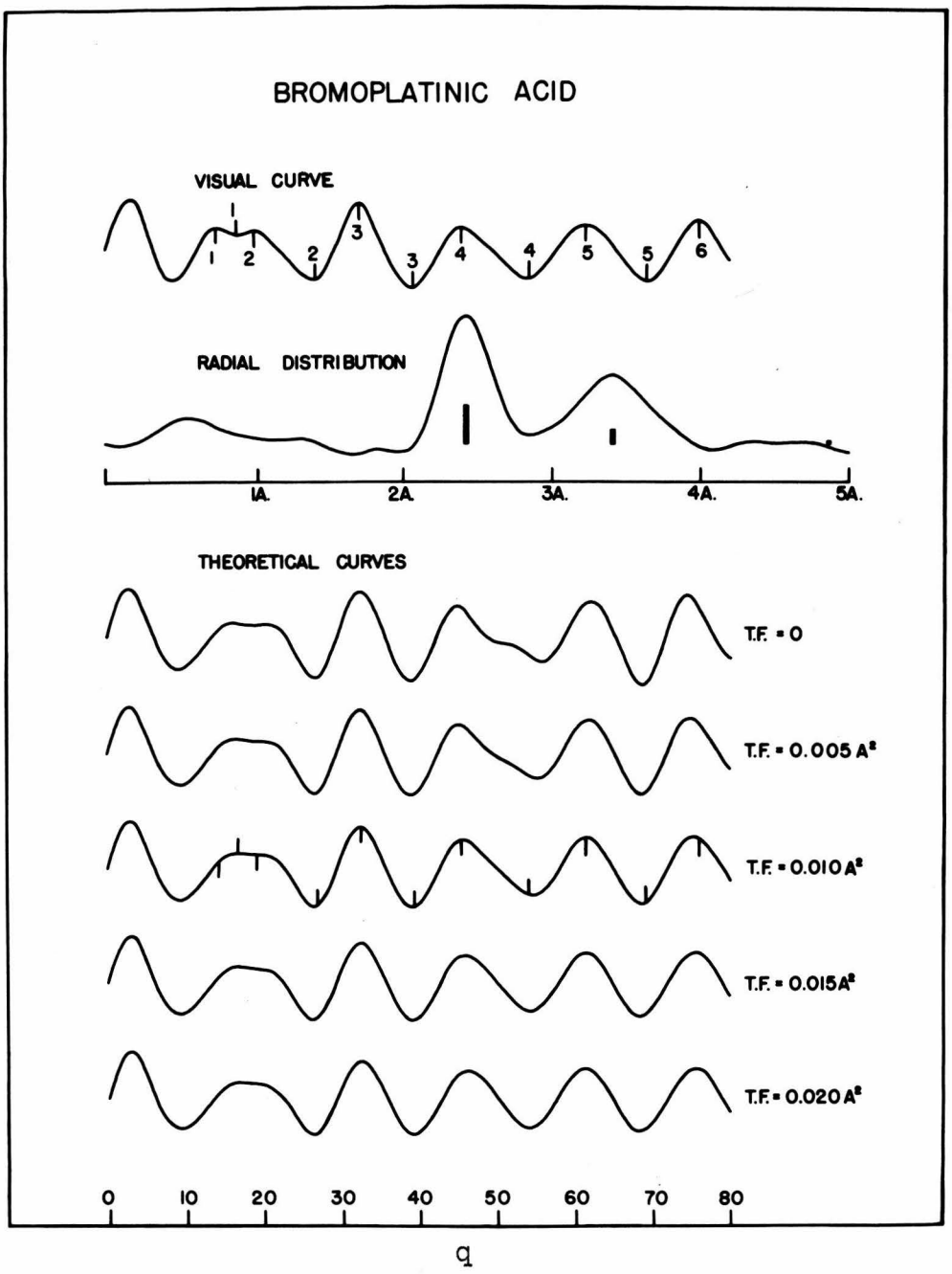
BROMOPLATINIC ACID
VISUAL CURVE
1
2
2
3
3
4
4
5
5
6
RADIAL DISTRIBUTION
1A.
2A.
3A.
4A.
5A.
THEORETICAL CURVES
T.F. = 0
T.F. = 0.005 A²
T.F. = 0.010 A²
T.F. = 0.015 A²
T.F. = 0.020 A²
0
10
20
30
40
50
60
70
80
q

Figure 4

following summation was then made using the International Business Machine Tabulator (see Equation 12):

$$D_o(r') = \sum_{q=1}^{80} I'_o(q)\, e^{-a'q^2} \sin(0.03\, r' q) \qquad 13$$

where a' is chosen so that $e^{-a'q^2} = 0.1$ at $q = q_{max} = 80$. The cards are punched so that the values of this function are tabulated from r' = 0 to $r' = \frac{143\pi}{10}$, in steps of $\frac{\pi}{10}$. Thus, the tabular interval is $\frac{70}{4\pi} \times 0.03 \times \frac{\pi}{10} = 0.0525$ Å. Two pronounced maxima are observed, one at 2.43 Å and a weaker and broader one at 3.41. Since $\frac{3.41}{2.43} = 1.403$, which is very nearly $\sqrt{2}$, the octahedral model is clearly indicated, with the Pt - Br distance equal to 2.43 Å.

In calculating theoretical intensity curves, the amplitudes of the Pt - Br terms are put equal to a constant, k. The Br - Br amplitudes are then given to a satisfactory degree of approximation by $k \frac{r(Br - Br)}{r(Pt - Br)} \times \left(\frac{f(Br)}{f(Pt)}\right)_{average}$. The average value of the ratio $\frac{f(Br)}{f(Pt)}$ over the observed angular interval is equal to 0.375, which was estimated from the atomic scattering factors given in the Internationale Tabellen zur Bestimmung von Kristallstrukturen. In order that comparisons between observed and calculated curves can be easily made, it is convenient to have the tabular interval for the theoretical curves, Δq, equal to 1. Because of the way in which we have defined q and the way in which the cards are punched, this will be the case if we set the frequency for each term, u_{ij}, equal to 4/7 r_{ij}. Substituting the values for r_{ij} and s in Equation 8 gives

$$I'_c(q) = \sum_i \sum_j \left(\sum_{k=-N}^{N} \frac{A_{ij}}{2\sqrt{\pi a_{ij}}} e^{-\frac{(k\Delta r)^2}{4a_{ij}}} \sin \frac{\pi q}{10}(u_{ij} + k\Delta u) \right)$$

$$+ \sum_l \sum_m A_{lm} \sin \frac{\pi q}{10} u_{lm} \qquad 14$$

The tabulating machine calculates the values of this function for q = 1, 2, 3 . . . . 144. For all the calculations in this Thesis which involved temperature factors, Δu was equal to 0.05, or Δr equal to 0.0875 Å.

In Figure 4 theoretical curves are given with the temperature factors of the Br - Br terms equal to 0, 0.005, 0.010, 0.015, and 0.020 $Å^2$. With no temperature factor there is a pronounced shoulder on the outside of the fourth maximum instead of the asymmetry which is indicated by the visual curve. The fourth minimum is also farther to the right than observed, and the separation of the fourth and fifth maxima is too great. These disagreements can all be rectified by applying a temperature factor to the Br - Br distances. A temperature factor of 0.010 $Å^2$ gives good agreement with the visual intensity curve with the exception of the first and second maxima. Since the first peak on the theoretical curve might well give the appearance of a doublet as indicated on the visual curve, the principal disagreements are in the measurements. It will be remembered, however, that it is in this part of the curve that effects due to intermolecular distances will be observed, if they are to have any effect at all. Moreover, on practically all of the photographs examined, there has been a general tendency to

measure the first maximum too close to the center of the film. Table 2 gives a comparison of the maxima and minima observed on the film and on the theoretical curve with a 0.010 Å^2 temperature factor. Table 3 gives the average value of q_{calc}/q_{obs} for the

Table 3

Temperature factor	0	0.005	0.010	0.015	0.020
Average q_{calc}/q_{obs} (five feature)	1.001	0.999	0.999	0.999	1.001
Average deviation (five features)	1.0%	0.7%	0.3%	0.4%	0.5%

five most accurately measured features and also the average percent deviation of q_{obs} from q_{calc} for each of the models. In each case the most probable Pt - Br distance is 2.43 Å. This is in good agreement with the sum of the octahedral radii, which is 2.45 Å.

2. Chloroplatinic Acid

Dr. J. M. Sturdivant had obtained two diffraction photographs of a saturated aqueous solution of chloroplatinic acid before the work described in this Thesis was begun. The apparatus used was nearly identical with that described in section B. These photographs are labeled 5/10/38, film distance of 75 mm; and 6/4/38, film distance of 50 mm. Using these photographs, the structure of chloroplatinic acid has been determined. Dr. Sturdivant informs me that there is some doubt as to the exact film distances and that no check on the wavelength by means of a powder photograph is on record. Hence, the parameter which has been determined from these films might be somewhat in

error. However, the observed data are in accord with the octahedral structure of the chloroplatinate ion and are therefore presented as an additional indication of the possibility of using the solution method for structure determinations.

Table 4

Feature max	Feature min	q_{obs}	q_{calc}	$\frac{q_{calc}}{q_{obs}}$	$\left(\frac{q_{calc}}{q_{obs}}\right) / \left(\frac{q_{calc}}{q_{obs}}\right)_{average}$
1		19.1	18.4	(0.963)	(0.954)
	1	27.8	26.6	(0.959)	(0.950)
2		33.2	33.4	1.006	0.997
	2	39.8	40.5	1.017	1.008
3		46.7	47.6	1.019	1.010
	3	54.9	55.8	1.016	1.007
4		63.0	63.1	1.002	0.993
	4	71.0	70.5	0.993	0.984
5		78.4	77.7	(0.991)	(0.982)
Average (6 features) ---				1.009	1.000
Average absolute deviation					0.8%

The visual intensity curve, radial distribution integral, and theoretical curves are given in Figure 5. The radial distribution function has a very prominent peak at 2.37 Å and a considerably smaller one at 3.35 Å. This is in accord with the octahedral model. The theoretical curves were calculated with the Pt - Cl distance equal to 2.37 Å. The procedure for calculating these curves was the same as that used for the

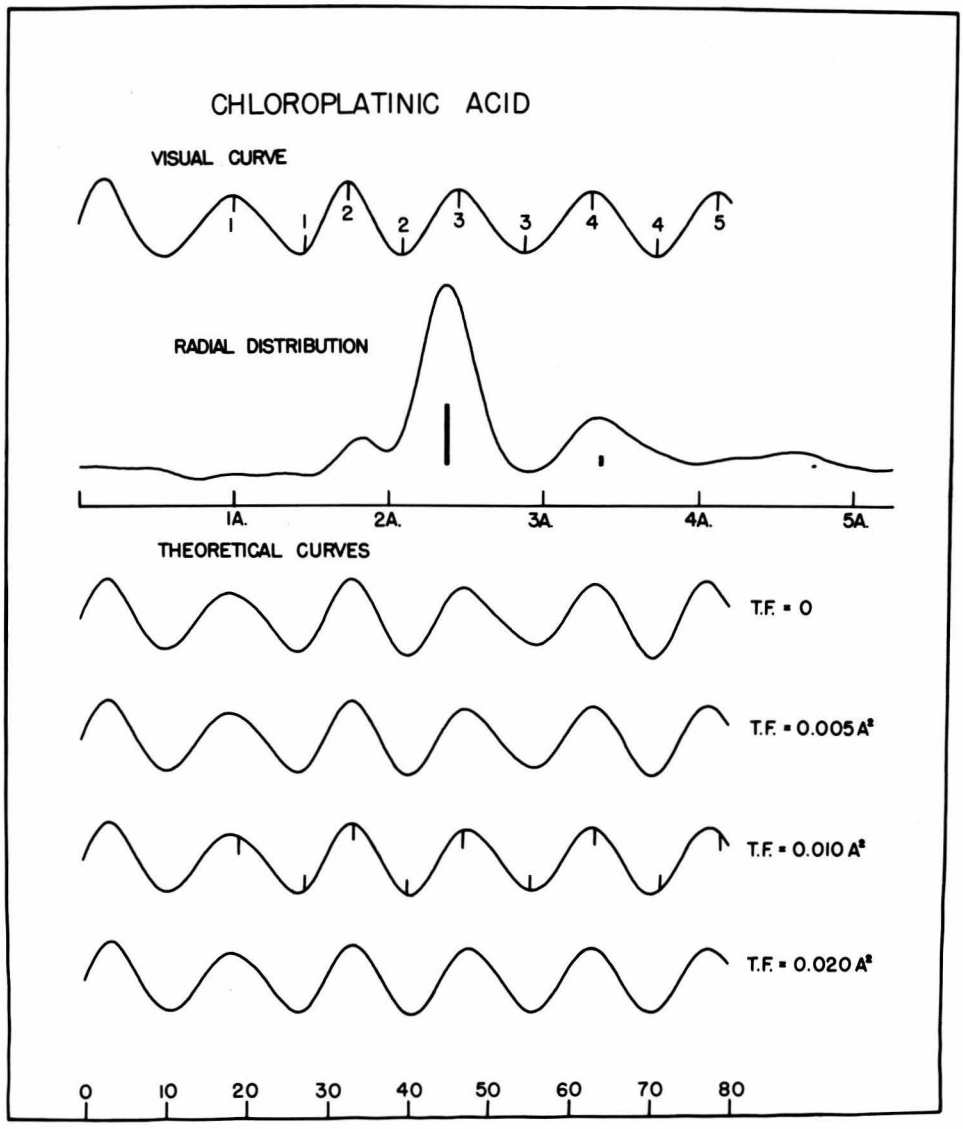
CHLOROPLATINIC ACID
VISUAL CURVE
1
1
2
2
3
3
4
4
5
RADIAL DISTRIBUTION
1A.
2A.
3A.
4A.
5A.
THEORETICAL CURVES
T.F. = 0
T.F. = 0.005 A²
T.F. = 0.010 A²
T.F. = 0.020 A²
0
10
20
30
40
50
60
70
80
q

Figure 5

bromoplatinate ion. The curves with Cl - Cl temperature factors of 0.005 and 0.010 $Å^2$ are in best agreement with the visual curve. However, the difference between any of these curves is not very great because of the relatively small contribution of the Cl - Cl terms. Table 4 gives the comparison between the observed and calculated q values of the maxima and minima. Since the observed average of q_{calc}/q_{obs} is 1.009, the best parameter is 1.009 x 2.37 = 2.39 Å. This is not in good agreement with the octahedral radii sum, which is 2.30 Å. The Pt - Cl distance in K_2PtCl_6 (12) is 2.33 Å.

D. Lower Halide Complexes of Columbium and Tantalum

1. Preparation and Chemistry

In 1907 Chabrié (13) prepared a lower chloride of tantalum by the reduction of tantalum pentachloride with sodium amalgam. He assigned to this compound the formula $TaCl_2 \cdot 2H_2O$ on the basis of a single analysis. This compound was somewhat soluble in water, forming a dark green solution from which it could be crystallized in small, hexagonal crystals. Four years later Chapin (14) prepared a compound which was identical in appearance with Chabrié's chloride by the reduction of tantalum pentabromide with sodium amalgam. Careful analyses indicated that the formula of this compound is $Ta_6Br_{14} \cdot 7H_2O$. Synthesis and analysis of Chabrié's chloride indicated the analogous formula, $Ta_6Cl_{14} \cdot 7H_2O$. Chapin carried out boiling point measurements of a solution of the bromide in propyl alcohol which indicated a molecular weight corresponding to $Ta_6Br_{14} \cdot 7H_2O$.

Freezing point depression measurements in aqueous solution gave a value one-third as great. This fact led Chapin to the conclusion that two bromide ions are produced in aqueous solution as well as the complex ion $(Ta_6Br_{12})^{++}$. This hypothesis is supported by the fact that two, and only two, of the bromine atoms can be replaced by other halogens by evaporating a solution of the compound in dilute aqueous hydrochloric or hydriodic acid. The compound $(Ta_6Br_{12})(OH)_2 \cdot 10H_2O$ is formed in a slightly alkaline solution.

Other workers have also investigated the chemistry of these rather interesting compounds. Lindner and Feit (15) prepared the complex chloride by reducing tantalum pentachloride with lead powder at red heat in a nitrogen atmosphere. They carried out analyses which led them to believe that the formula of this compound is $H_2Ta_6Cl_{14} \cdot 8H_2O$. Quantitative oxidation with potassium permanganate was used to determine the oxidation number of tantalum, which they concluded was +2. This is in disagreement with the conclusions of Ruff and Thomas (16). These workers claim that the same complex is produced when a lower chloride of tantalum, to which they ascribe the formula $TaCl_3$, is dissolved in dilute hydrochloric acid and evaporated. They also measured the valence of tantalum by observing the volume of hydrogen liberated when a weighed quantity of the compound was warmed in basic aqueous solution. They report an oxidation number of +3 and claim that the correct formula is $Ta_6Cl_{14}O_2 \cdot 6H_2O$. As additional evidence they cite the fact (observed also by Lindner and Feit) that only six molecules of water are lost on

mild heating. I do not think that this is very significant evidence in favor of their formula, however, since this fact might well be explainable in terms of the structure of the compound. In view of the above disagreements, the valence of this complex compound remains in doubt. A structure determination is still quite possible, however, since the number of halogen and tantalum atoms per molecule is known.

H. S. Harned (17) prepared a compound which his analyses indicated was $Cb_6Cl_{14}\cdot 7H_2O$. He also showed by potentiometric titration with silver nitrate solution that two of the fourteen chlorine atoms are easily removed. The compounds $Cb_6Cl_{12}(OH)_2\cdot 8H_2O$ and $Cb_6Cl_{12}Br_2\cdot 7H_2O$ were also prepared. Therefore this compound seems to be analogous to the $Ta_6Cl_{14}\cdot 7H_2O$ and $Ta_6Br_{14}\cdot 7H_2O$ described by Chapin.

Dr. Harned was kind enough to lend the Institute a considerable quantity of his chloride which was used for the structure determination described herein.

I prepared the complex lower chloride of tantalum by reduction of the pentachloride by granular lead in a nitrogen atmosphere at a dull red heat. The pentahalide was prepared by passing a stream of chlorine saturated with carbon tetrachloride vapor over an intimate mixture of tantalum pentoxide and charcoal maintained at a full red heat in a silica tube. The volatile pentachloride was allowed to condense at the cool end of the tube. It was then distilled into a silica bulb containing granular lead, where the reduction was carried out. After completion of the reduction, the complex chloride was leached

out of the resulting mass with hot, dilute hydrochloric acid. It was obtained in small, black needles by evaporation of the resulting solution in vacuum. The complex lower bromide was prepared in a very similar manner. Tantalum pentabromide was made by passing a stream of nitrogen saturated with bromine over a red hot mixture of charcoal and tantalum pentoxide. The reduction was also carried out with granular lead, and hydrobromic acid was used to extract the desired compound.

Attempts were made to synthesize the analogous columbium bromide by reduction of columbium pentabromide. Both lead and 3 percent sodium amalgam were tried as reducing agents, but in neither case was a significant quantity of the desired compound obtained.

None of the complex halides described above is soluble enough in water to enable one to obtain suitable solution photographs. They are, however, extremely soluble in ethanol. Therefore this solvent was used exclusively. Since these compounds are presumably not ionized in ethanol solution, the principal diffracting molecules contain fourteen halogen and six tantalum atoms.

In the following discussion the formulae of these complexes will be written in the form $Ta_6Cl_{14}\cdot 7H_2O$.

2. The Structure of the (Cb_6Cl_{12}) Group

The four following diffraction photographs were made of a concentrated alcoholic solution of $Cb_6Cl_{14}\cdot 7H_2O$:

Date	Film Distance	Sample Thickness	Exposure
8/24/48	5.225 cm	0.8 mm	530 m.a.h.
9/27/48	" "	0.8 mm	1950 m.a.h.
11/19/48	" "	0.7 mm	2000 m.a.h.
11/30/48	" "	0.7 mm	2120 m.a.h.

The last two photographs were used in preparing the visual curve since they were considerably better than the first two.

The visual curve and radial distribution function are shown in Figure 7. In this investigation and in those following, the units and procedure used in calculating the radial distribution and theoretical curves are the same as those described in the investigation of bromoplatinic acid.

The radial distribution function has two incompletely resolved peaks in the vicinity of 2.4 and 2.9 Å, the latter being considerably higher than the former. There is also a prominent peak at 3.92 Å and a rather low one at approximately 5 Å. In deciding on a trial structure it is necessary to make a choice which is consistent with the chemistry of this compound and with the radial distribution curve. It is evident from chemical considerations that two of the chlorine atoms cannot be related by symmetry to the other twelve. A structure which suggests itself is the following: Place the six columbium atoms at the corners of a regular octahedron whose edges are 2.9 Å long. Then place twelve chlorine atoms on the perpendicular bisectors of the edges so that the columbium-chlorine distances are approximately 2.4 Å (see Figure 6). A calculation then shows that the most prominent distances will be

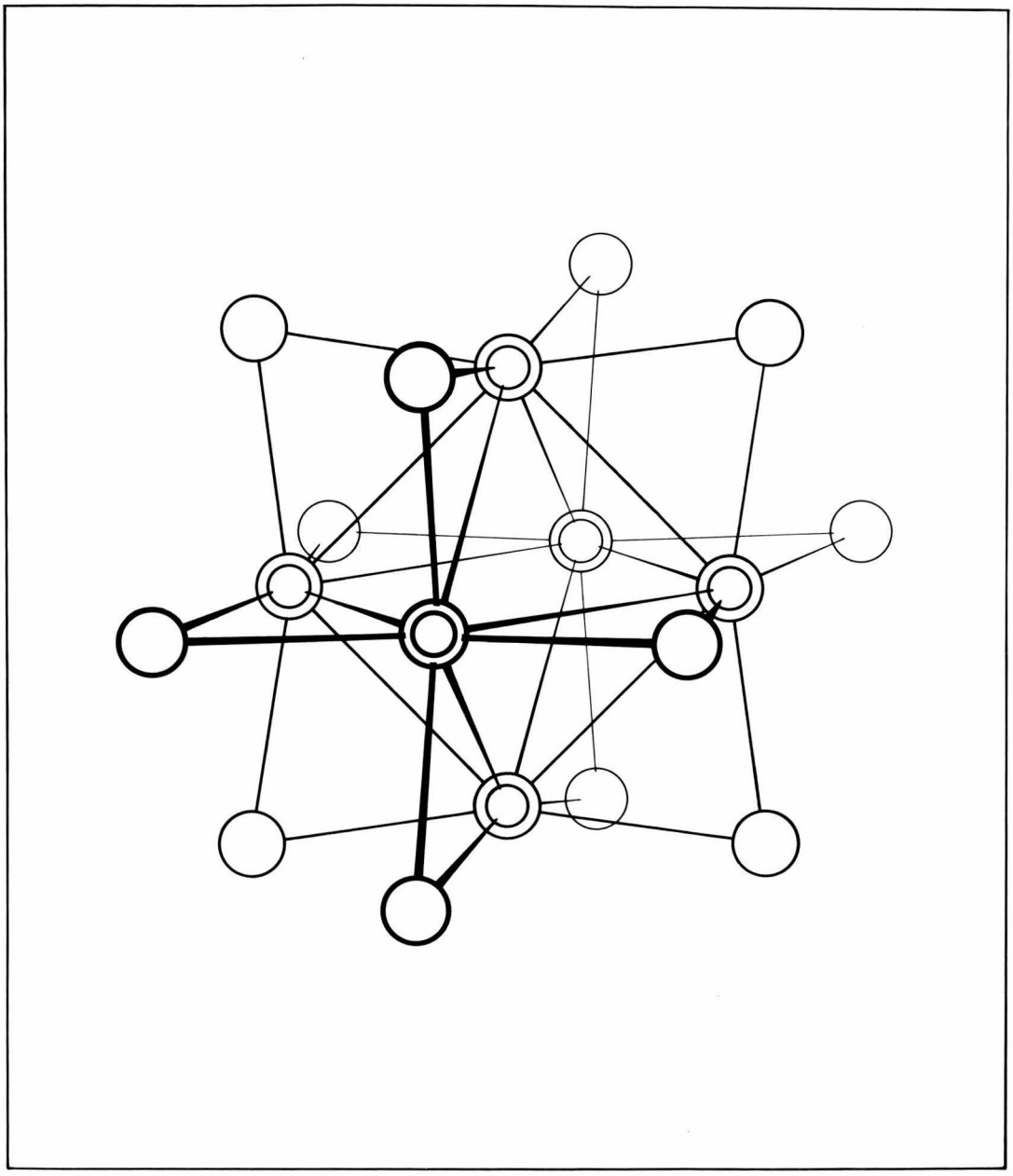

Figure 6

Structure of the (M_6X_{12}) Group in

$Cb_6Cl_{14}\cdot 7H_2O$, $Ta_6Br_{14}\cdot 7H_2O$, and $Ta_6Cl_{14}\cdot 7H_2O$

Double circles - metal atoms
Single circles - halogen atoms

Designation	Description
r_1	Twelve Cb - Cb distances at 2.9 Å
r_2	Twenty-four Cb - Cl distances at 2.4 Å
r_3	Twenty-four Cb - Cl distances at 3.95 Å
r_4	Twenty-four Cb - Cl distances at 5.0 Å

This structure meets all of the requirements of the known chemistry of the molecule and of the radial distribution function. No attempt has been made to account for the two remaining chlorine atoms since it is evident that their direct effect on the intensity function will be quite small. It is possible, however, that they could cause enough distortion of the above symmetrical structure to be significant.

With the assumption of cubic symmetry there are only two parameters to be determined, a scale parameter and the ratio (r_1/r_2) of the shortest Cb - Cb to the shortest Cb - Cl distance. The following theoretical curves were calculated and are shown in Figure 7,

Designation	$(r_1/r_2) = R$
A	1.137
B	1.168
C	1.187
D	1.207
E	1.227

These curves were calculated with $\left(\frac{f_{Cl}}{f_{Ta}}\right)_{average} = 0.348$. The amplitudes of the various terms are then given by

$$A_{Cb\text{-}Cb} = A_{r_1} \times \frac{r_1}{r_{Cb\text{-}Cb}} \times \frac{N_{Cb\text{-}Cb}}{12}$$

$$A_{Cb\text{-}Cl} = 0.348\, A_{r_1} \times \frac{r_1}{r_{Cb\text{-}Cl}} \times \frac{N_{Cb\text{-}Cl}}{12}$$

$$A_{Cl\text{-}Cl} = (0.348)^2 A_{r_1} \times \frac{r_1}{r_{Cl\text{-}Cl}} \times \frac{N_{Cl\text{-}Cl}}{12}$$

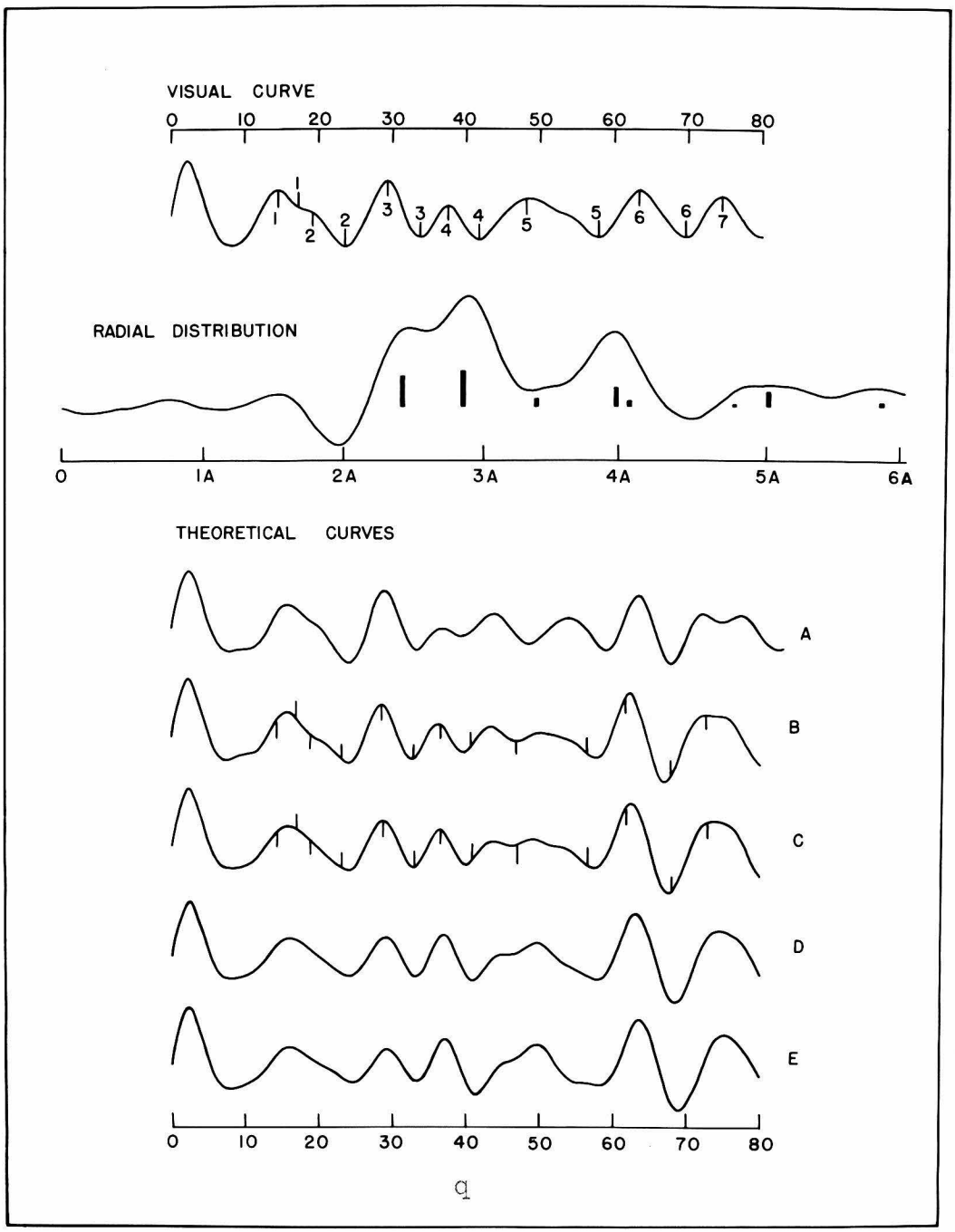

Figure 7

Data on $Cb_6Cl_{14}\cdot 7H_2O$

where A_{x-y} is the amplitude of the distance of length r_{x-y} which occurs N_{x-y} times in the molecule. A_{r_1}, the amplitude of the shortest Cb - Cb term, was arbitrarily given a value of 50.

The best agreement with the visual curve is an interpolation between curves B and C. There are, however, certain objections to all of these curves. In curve B the fourth minimum is not as wide and deep as the appearance of the film would seem to suggest. Moreover, the broad feature, which I have called the fifth maximum, contains a minimum which one might expect to see. These troubles seem to be at least partially corrected by increasing R slightly, as in curve C; but another difficulty then appears. The fourth maximum becomes more prominent than it probably should be. This maximum appears on the film to be considerably lower than the average of the third and fifth maxima. A way of improving this situation is suggested by observing the radial distribution function. The peak at 5 Å is considerably flatter and lower than it would be in the case of a symmetrical model without temperature factors. A calculation also shows that this high frequency term has one maximum just to the right of the fourth minimum and another very close to the fourth maximum. Hence, applying a temperature factor to this term would both increase the width of the fourth minimum and decrease the height of the fourth maximum. Since it is not likely that r_4 will have a fairly large temperatus factor and r_3 none, it becomes necessary to investigate the effect of a temperature factor on both of these distances. A number of theoretical curves were calculated in which both of these

temperature factors were varied; they are shown in Figures 8 and 9. In making these calculations no temperature factors were applied to the long Cb - Cb distance or to the Cl - Cl distances. These terms contribute but little to the scattering curve. The two least important Cl - Cl terms were omitted completely. The parameters used to calculate each of these curves can be found by referring to Figure 10, in which the position of each curve is shown graphically. The shaded area represents the region of acceptability. The full, curved line in each diagram is the locus of the best values of R. The large dot represents the best parameters for each value of the temperature factor ratio.

Examination of the theoretical curves in Figures 8 and 9 shows that the temperature factor on the longest Cb - Cl distance helps considerably. A temperature factor as small as 0.005 Å^2 would result in considerable improvement. However, too large a temperature factor on r_3 has a tendency to make the fourth minimum too shallow and has an adverse effect on the shape of the broad fifth maximum; the most that can be allowed for this temperature factor is about 0.005 Å^2. Temperature factors of 0.005 - 0.010 Å and 0.002 - 0.005 Å^2 for r_4 and r_3, respectively, give satisfactory agreement with the visual curve and are also consistent with the work done on bromoplatinic acid. It is not possible to assign any special physical significance to the temperature factors discussed above since there are at least three possible explanations for them: (1) the presence of considerable thermal motion; (2) small splitting of these distances due to distortions introduced by the two remaining

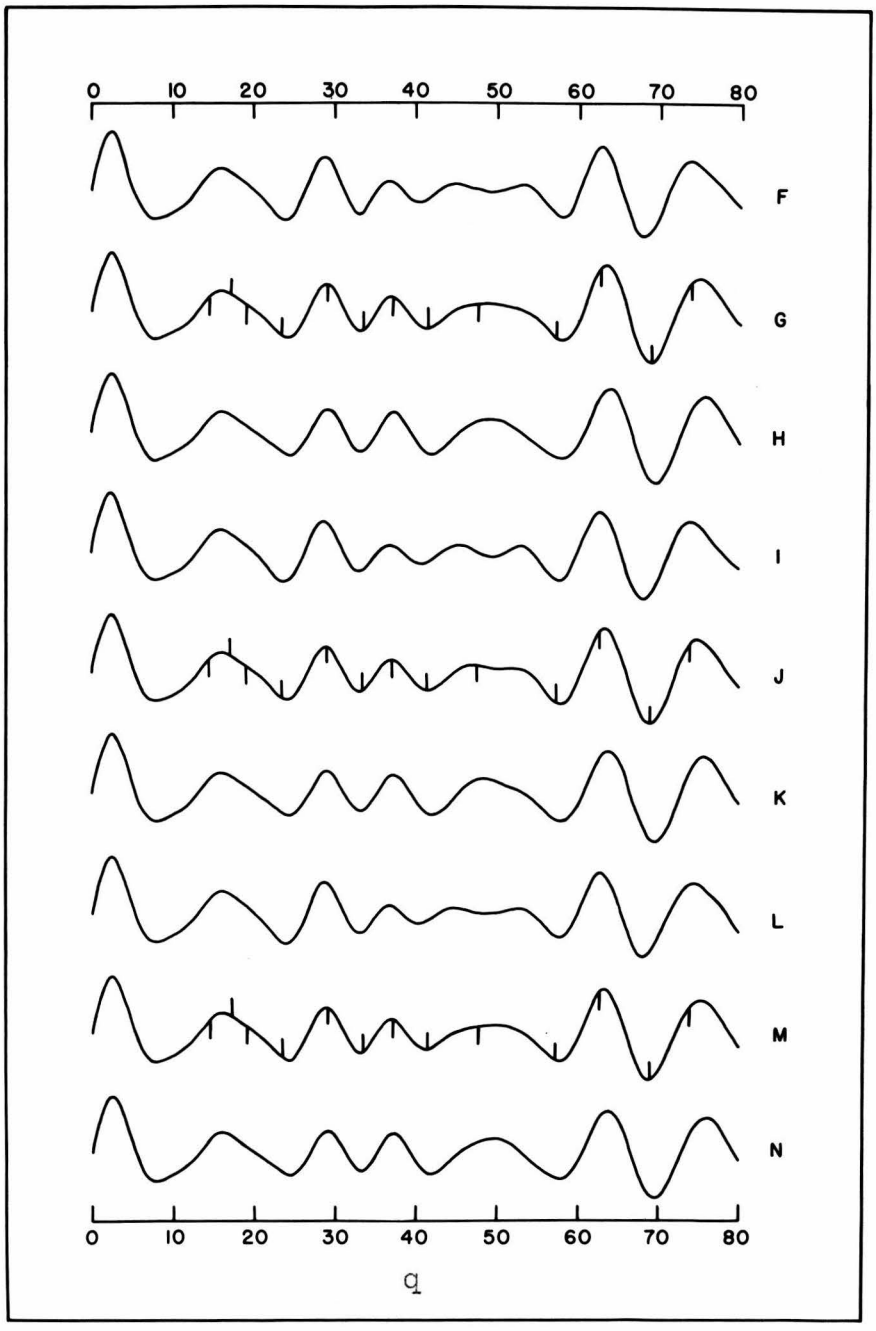

Figure 8

Theoretical Curves for the (Cb_6Cl_{12}) Group

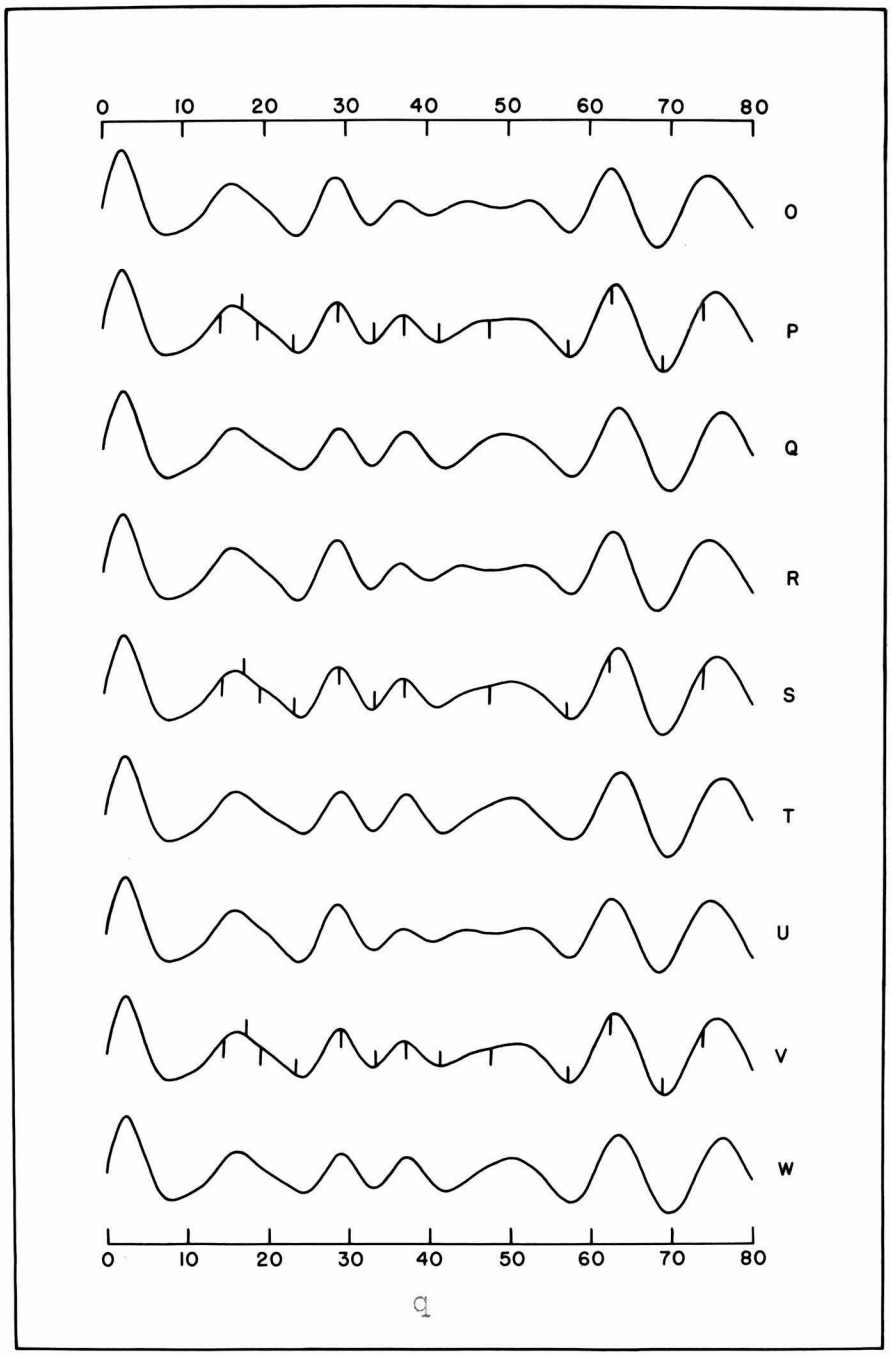

Figure 9

Theoretical Curves for the (Cb_6Cl_{12}) Group

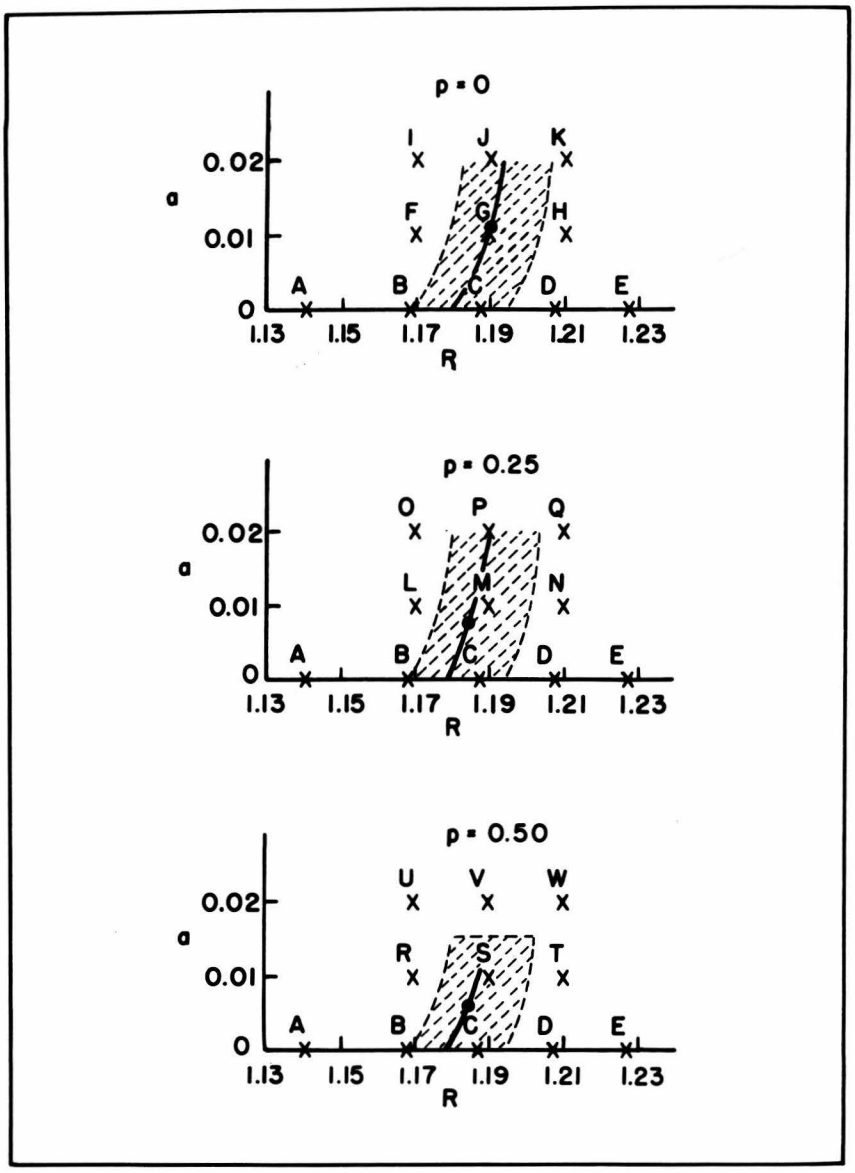

Figure 10

Parameters of the Theoretical Curves

Calculated for the (Cb_6Cl_{12}) Group

a = Temperature factor of r_4
p = Ratio of temperature factor of r_3 to that of r_4

chlorine atoms, and (3) decrease of resolution due to the experimental arrangement. Any one of these, or a combination of them, might well cause a real or apparent temperature factor.

Fortunately, the choice of the best value of R and the scale factor vary but little with the temperature factors assigned to the longer distances. A comparison of the observed and calculated positions of the maxima and minima will be found in Table 5. The scale factor has been adjusted in each case so that the average value of q_{calc}/q_{obs} for the six most reliably measured features is equal to 1.000. I have concluded that the best choice of parameters is the following:

Shortest Cb - Cb	2.85 Å
Shortest Cb - Cl	2.41 Å
T. F. of longest Cb - Cl	0.005 - 0.010 $Å^2$
T. F. of next to the longest Cb - Cl	0.002 - 0.005 $Å^2$

The four principal sources of error are (1) qualitative errors in drawing the observed intensity curve, (2) errors in measuring the radii of the rings, (3) possible errors in the mean wave length, and (4) spectral impurity of the monochromatized beam, which might cause distortions in the appearance of the photograph. The limit of error due to the first two sources is estimated from the region of acceptability on Figure 10 and from the average deviations in Table 5 to be approximately ± 0.05 Å for r_1 and r_2. A reasonable estimate of the total limit of error is 0.07 Å.

Table 5

max	min	q_{obs}	q_{calc} B	q_{calc} C	q_{calc} M	q_{calc} S	q_{calc}/q_{obs} B	q_{calc}/q_{obs} C	q_{calc}/q_{obs} M	q_{calc}/q_{obs} S
1		14.7	16.1	16.2	16.2	16.3	(1.096)	(1.099)	1.105	(1.110)
	1	17.4	-	-	-	-	-	-	-	-
2		19.3	-	-	-	-	-	-	-	-
	2	23.7	24.9	24.7	24.5	24.5	(1.050)	(1.032)	(1.035)	(1.035)
3		29.4	29.4	29.4	29.2	29.4	1.000	1.000	0.995	1.000
	3	33.8	33.6	33.7	33.4	33.5	0.995	0.998	0.989	0.990
4		37.6	37.3	37.4	37.3	37.5	0.992	0.994	0.994	0.998
	4	41.9	40.9	41.1	41.8	41.7	0.977	0.981	0.997	0.995
5		48.2	-	-	-	-	-	-	-	-
	5	57.9	59.4	58.5	58.4	58.5	1.025	1.013	1.009	1.000
6		63.3	64.0	64.0	63.8	64.2	1.012	1.012	1.009	1.014
	6	69.7	69.0	69.4	69.4	69.9	(0.990)	(0.994)	(0.996)	(1.002)
7		74.6	75.5	75.8	76.0	76.6	(1.012)	(1.015)	(1.019)	(1.027)
Average abs. deviation (6 features)							0.012	0.009	0.007	0.005
Parameters:										
Shortest Cb - Cb							2.84	2.85	2.86	2.84
Shortest Cb - Cl							2.44	2.40	2.40	2.39

3. The Structure of the (Ta_6Br_{12}) Group

Four diffraction photographs of a concentrated solution of $Ta_6Br_{14}\cdot 7H_2O$ in ethanol were obtained:

Date	Film Distance	Sample Thickness	Exposure
6/21/48	5.33 cm	0.7 mm	2860 m.a.h.
7/7/48	5.218 cm	0.7 mm	2020 m.a.h.
7/12/48	5.218 cm	0.7 mm	660 m.a.h.
10/12/48	5.21 cm	0.8 mm	1260 m.a.h.

The last photograph was considerably superior to the others.

The visual curve and radial distribution function obtained from it are shown in Figure 11. In the latter curve there is a very high, broad maximum at 2.72 Å and smaller maxima at 3.64 Å, 4.16 Å, and 5.25 Å. The similarity to the radial distribution function for $Cb_6Cl_{14}\cdot 7H_2O$ is immediately apparent. However, in this case all of the metal-halogen distances are longer because of the larger radius of bromine. The shortest Ta - Ta and Ta - Br distances are so close together that they are unresolved. The same model is assumed as for the (Cb_6Cl_{12}) group, the tantalum atoms being at the corners of an octahedron and the bromine atoms on the perpendicular bisectors of the edges (see Figure 6). Theoretical curves were calculated for the following models:

Designation	$(r_1/r_2) = R$
A	1.066
B	1.082
C	1.098
D	1.114
E	1.132
F	1.150

which are shown on Figure 11. The average value of the ratio of the scattering factor of bromine to that of tantalum was estimated to be 0.40. The procedure used for calculating amplitudes was the same as that described in the last section.

In comparing these curves it must be kept in mind that the position and shape of the low third maximum is very difficult to determine. It is certain that this peak is very much lower than the fourth maximum and that the second minimum is considerably deeper than the third. Indeed, it cannot be said

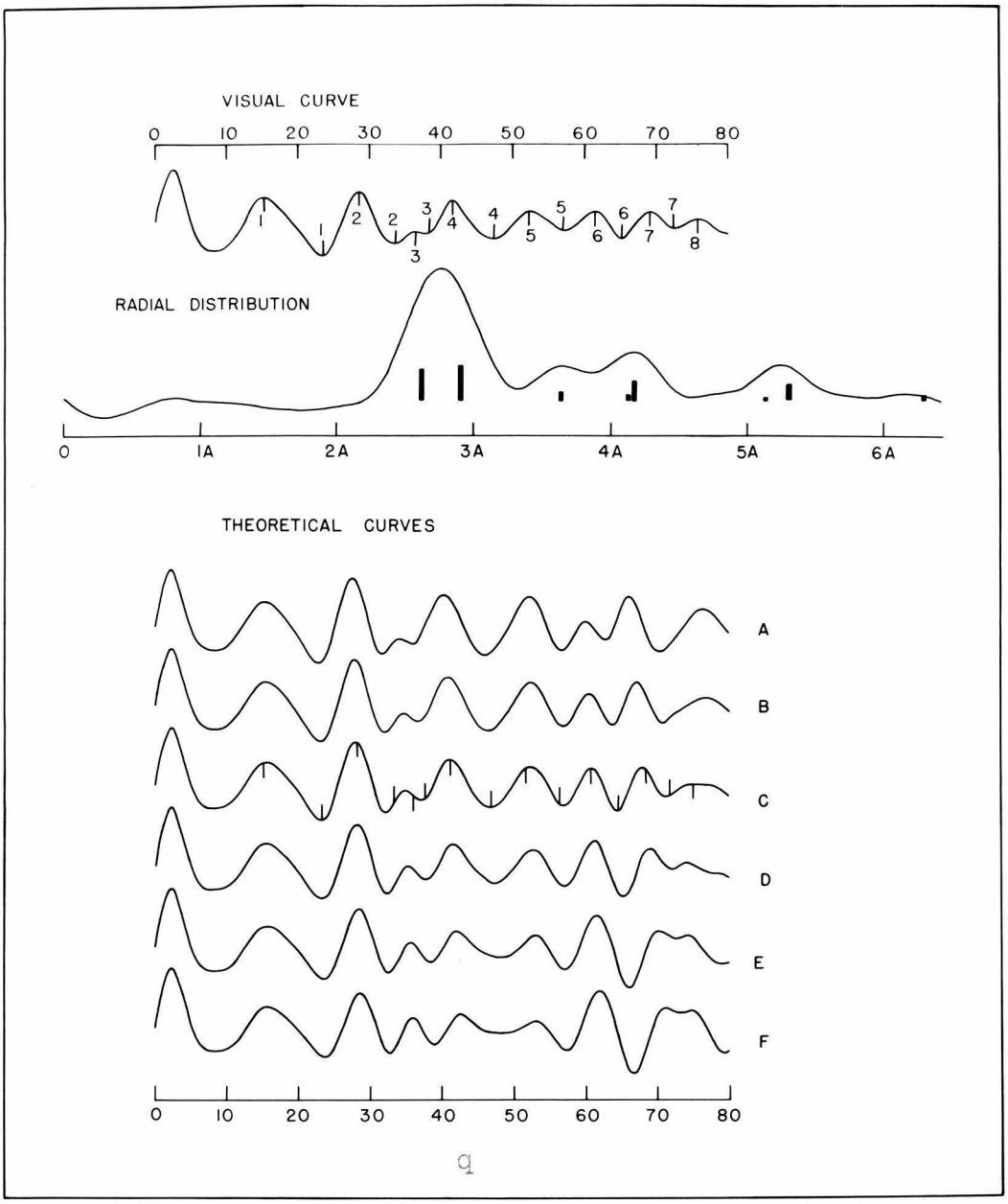

Figure 11

Data on $Ta_6Br_{14}\cdot 7H_2O$

with certainty that a minimum is actually present between the indicated third and fourth maxima. The fourth maximum appears to be higher than the fifth, while the fifth, sixth, and seventh maxima appear to be of approximately equal height. However, some disagreement with the latter observation must not be considered important. The sixth minimum appears to be definitely deeper than the fifth. It is extremely difficult to see the eighth maximum, and, since it occurs quite far out on the film, one cannot even be sure that it is present.

Model C gives the best agreement with the visual curve. Model E cannot be accepted because of height of the third and sixth maxima and depth of the third minimum. Model D, however, is considered acceptable. Model B gives poor agreement and represents the limit of acceptability in this direction. In this curve the fifth maximum is too high and the sixth minimum too shallow compared to the fifth. Table 6 gives the observed and calculated (model C) positions of the maxima and minima. The scale factors have been adjusted to give an average deviation of zero for the eight most accurately measured features. A slight increase in R over that in model C seems desirable and the best parameters are taken to be 2.90 Å for the Ta - Ta and 2.63 Å for the Ta - Br distances.

In spite of the satisfactory agreement between observed and calculated intensity curves, we cannot yet be content with the above determination. In studying the chlorocolumbium and the bromoplatinate ions, the best agreement was obtained when appreciable temperature factors were applied to the longer distances.

We should, therefore, investigate the effect of such temperature factors on the theoretical intensity curves of the bromotantalum ion. Theoretical curves were calculated in which the longest (r_4) and next longest (r_3) Ta - Br distances were assigned various temperature factors; these curves are shown in Figure 12. The various parameters of each curve are shown graphically in Figure 13. In calculating these curves, the Br - Br distances were assigned the same temperature factors as the Ta - Br distance nearest them in length. Satisfactory curves could be obtained for any of the temperature factors considered. However, those curves for which the temperature factor ratio (p) is $\frac{1}{2}$ are slightly better than the others because the relative heights of the fourth and fifth maxima are in better agreement with the visual curve. The heavy full lines in Figure 13 represent the loci of the optimum values of R and the shaded area is the region of acceptability. It will be noticed that the most satisfactory value of R increases considerably as the temperature factor of r_4 increases. However, there is not an appreciable dependence on p, the temperature factor ratio, in the range considered. Examination of the theoretical curves does not enable one to choose optimum values for the temperature factors and hence decide on the most satisfactory value of R. However, previous experience has shown that a temperature factor of 0.05 - 0.01 for the longest Ta - Br distance is most reasonable. Therefore I choose as the following most probable parameters:

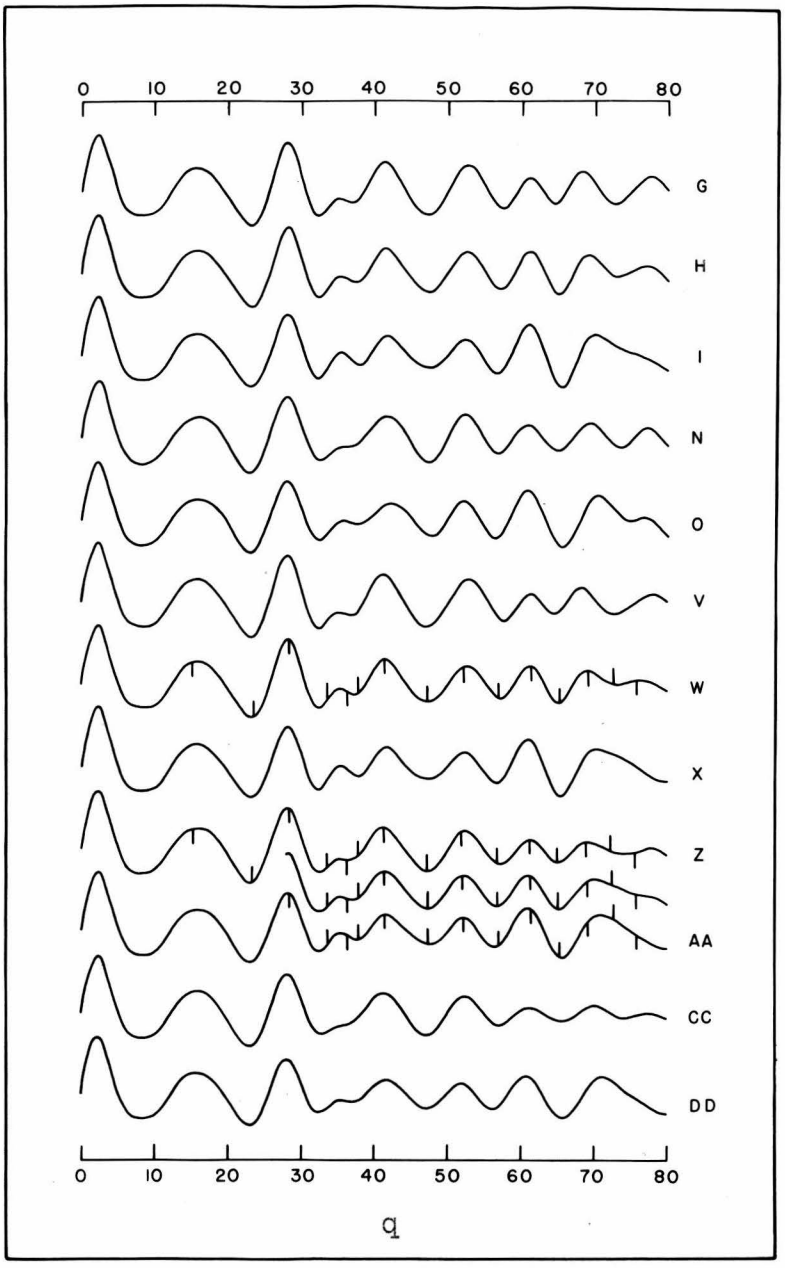

Figure 12

Some Theoretical Curves for the (Ta_6Br_{12}) Group

The curve between curves Z and AA
is an interpolation between these curves.

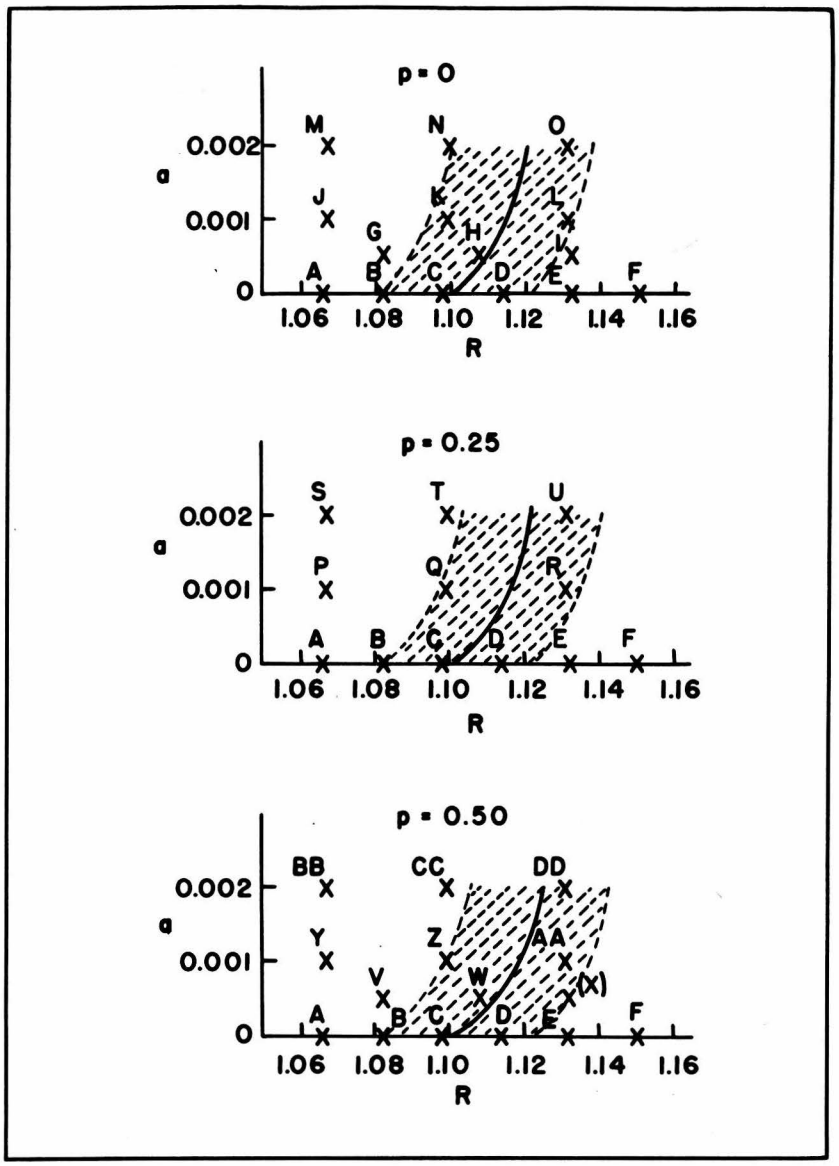

Figure 13

Parameters of the Theoretical Curves

Calculated for the (Ta_6Br_{12}) Group

a = Temperature factor of r_4
p = Ratio of temperature factor of r_3 to that of r_4

$R = 1.115 \pm 0.03$

	Distance, Å	Estimated Limit of Error, Å
Shortest Ta - Ta	2.92	0.07
Shortest Ta - Br	2.62	0.07

Table 6

max	min	q_{obs}	q_{calc}			q_{calc}/q_{obs}		
			W	Z	AA	W	Z	AA
1		15.2	15.9	16.4	16.0	(1.044)	(1.073)	(1.051)
	1	23.5	23.2	23.1	23.0	(0.986)	(0.982)	(0.978)
2		28.4	28.3	28.2	28.1	0.997	0.992	0.988
	2	33.6	32.3	32.7	32.3	(0.960)	(0.973)	(0.960)
3		36.4	35.3	35.6	35.5	(0.971)	(0.977)	(0.974)
	3	37.9	37.5	37.1	37.7	(0.985)	(0.979)	(0.994)
4		41.5	41.5	41.3	41.6	0.999	0.976	1.001
	4	47.3	47.4	47.5	47.7	1.001	1.005	1.007
5		52.1	52.6	52.6	52.0	1.010	1.009	0.999
	5	56.9	57.1	57.4	56.1	1.004	1.008	0.987
6		61.3	61.1	61.4	60.7	0.997	1.001	0.991
	6	65.1	64.9	65.2	65.4	0.997	1.001	1.007
7		69.0	69.1	69.3	70.6	1.002	1.004	1.003
	7	72.4	73.2	-	-	(1.011)	-	-
8		75.7	76.2	-	-	(1.007)	-	-
Average abs. deviation (8 features)						0.003	0.007	0.009
Parameters:								
		Shortest Ta - Ta				2.91	2.89	2.94
		Shortest Ta - Br				2.63	2.63	2.60

A comparison of observed and calculated positions of the maxima and minima are given in Table 6. In all cases, the scale parameter has been adjusted to make the average value of q_{calc}/q_{obs} equal to 1.000.

4. The Structure of the (Ta_6Cl_{12}) Group

The following diffraction photographs of $Ta_6Cl_{14}\cdot 7H_2O$ in ethanol solution were made:

Date	Film Distance	Sample Thickness	Exposure
4/27/48	5.42 cm	2.0 mm	2000 m.a.h.
5/8/48	5.42 cm	2.0 mm	462 m.a.h.
5/10/48	5.42 cm	2.0 mm	430 m.a.h.
10/5/48	5.21 cm	0.8 mm	990 m.a.h.

The last photograph was so much superior to the others that it was used almost exclusively for the structure determination. The visual intensity curve and radial distribution function calculated therefrom are shown in Figure 14. The latter curve is quite consistent with the structure proposed for the (Cb_6Cl_{12}) and (Ta_6Br_{12}) groups. The large maximum at 2.9 Å is the shortest Ta - Ta distance and the decided asymmetry on the inside of this peak corresponds to the shortest Ta - Cl distances. The prominent maximum around 4.0 Å and the very low one near 5 Å correspond to longer Ta - Cl and Ta - Ta terms and occur at the expected positions. In order to find the ratio of the shortest Ta - Ta to the shortest Ta - Cl distance (r_1/r_2), theoretical curves for the following models were calculated:

Designation	R	Temperature Factors r_4	r_3
A	1.137	0	0
B	1.169	"	"

Designation	R	Temperature Factors r_4	r_3
C	1.188	0	0
D	1.208	"	"
E	1.137	0.010 Å^2	0.005 Å^2
F	1.169	"	"
G	1.188	"	"
H	1.208	"	"
I	1.228	"	"
J	1.256	"	"

These theoretical curves are also shown in Figure 14. In calculating these curves a value of 0.19 was used for the average ratio of the scattering factor of chlorine to that of tantalum.

Theoretical curves were not calculated using temperature factors other than those given above, since these were found to be satisfactory for the (Cb_6Cl_{12}) and (Ta_6Br_{12}) structure determinations. Moreover, the tantalum-halogen terms are much less important in this case than in the others. It will be noticed, however, that better agreement with the visual curve is obtained when temperature factors are used. Model G gives the best agreement with the visual curve, and the optimum value of R is estimated to be 1.18 $\pm$ 0.04. For smaller values of R, as in model E, the shape of the third maximum and the position of the third minimum are in serious disagreement with what is observed. At larger values of R, the third maximum becomes too high, the third minimum too deep, and errors in the positions of the maxima and minima increase. A comparison between the observed and calculated positions of the maxima and minima are presented in Table 7 for models F and G. In each case, the scale parameter has been adjusted so that the average value of

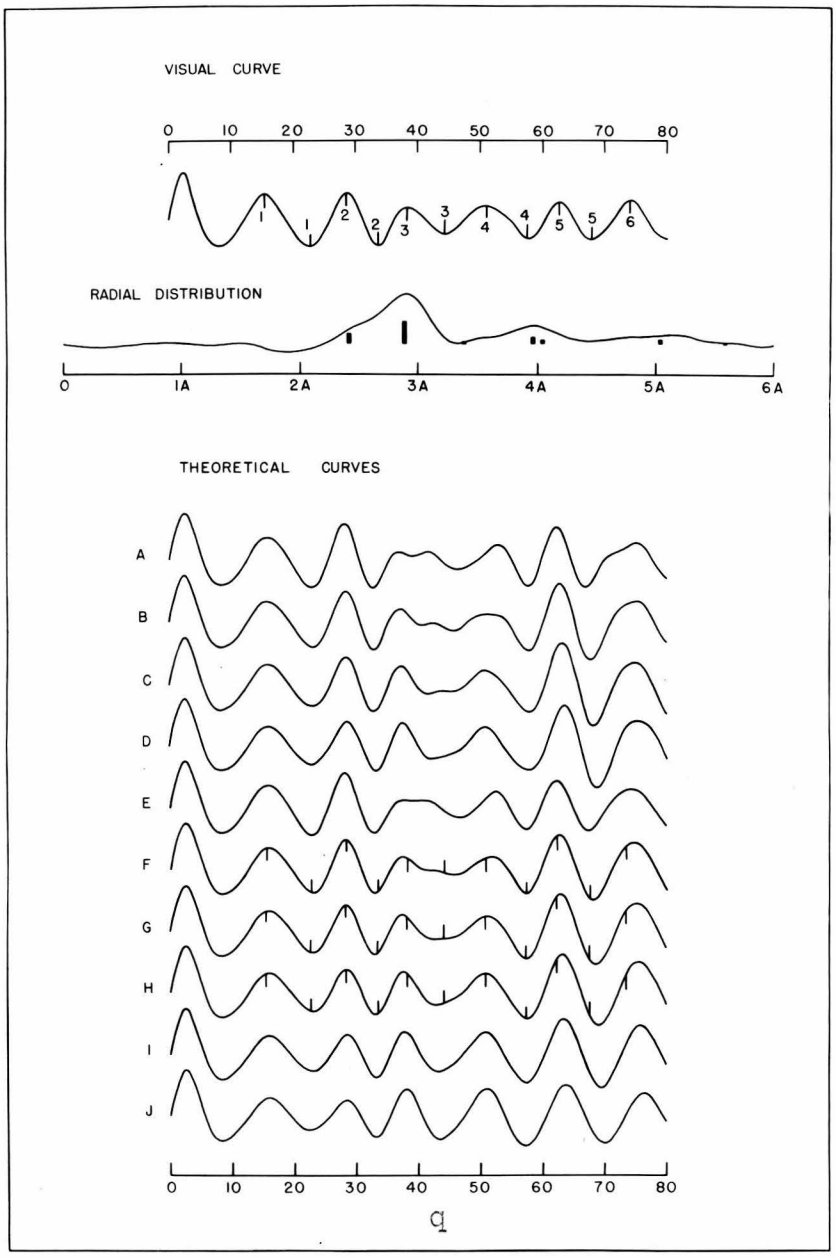

Figure 14

Data on $Ta_6Cl_{14}\cdot 7H_2O$

Table 7

max	min	q_{obs}	q_{calc} F	q_{calc} G	q_{calc}/q_{obs} F	q_{calc}/q_{obs} G
1		15.4	15.9	16.0	(1.033)	(1.039)
	1	22.7	23.0	23.0	(1.016)	(1.016)
2		28.4	28.4	28.5	1.000	1.003
	2	33.6	33.1	33.2	0.986	0.989
3		38.4	37.6	37.7	0.981	0.983
	3	44.4	45.8	44.1	(1.032)	(0.993)
4		51.1	52.0	51.3	1.019	1.005
	4	57.6	57.6	57.7	1.000	1.002
5		62.6	63.0	63.2	1.007	1.010
	5	68.0	68.5	69.0	1.008	1.016
6		74.0	75.2	75.7	(1.018)	(1.023)
Average abs. deviation (7 features)					0.010	0.009
Parameters:						
Shortest Ta - Ta					2.88 Å	2.88 Å
Shortest Ta - Cl					2.46 Å	2.42 Å

q_{calc}/q_{obs} for the six most reliably measured features is 1.000. The optimum parameters are the following:

	Distance, Å	Estimated limit of error, Å
Shortest Ta - Ta	2.88	0.05
Shortest Ta - Cl	2.44	0.10

5. Discussion and Summary

A summary of the parameters of the halide complexes of columbium and tantalum which have been investigated is given

below. Important distances in a somewhat similar complex of molybdenum determined by Cyrill Brosset (1) are also given.

Compound	Shortest M - M, Å	Shortest M - X, Å	Shortest X - X, Å	$\frac{1}{2}$(M - M) Å
$Cb_6Cl_{14}\cdot 7H_2O$	2.85	2.41	3.37	1.425
$Ta_6Cl_{14}\cdot 7H_2O$	2.88	2.44	3.41	1.44
$Ta_6Br_{14}\cdot 7H_2O$	2.92	2.62	3.64	1.46
$Mo_6Cl_8(OH)_4\cdot 14H_2O$	2.63(ave.)	2.56(ave.)		1.315

In the molybdenum compound the metal atoms are also at (or near) the vertices of a regular octahedron; the eight halogens, however, are located at the vertices of a circumscribed cube. Bonds are also formed with oxygen atoms at the vertices of a larger octahedron.

The deviation of the intermetallic radii of tantalum and columbium in these compounds from their average value (2.88 Å) is within the limits of error of this determination. Hence it cannot be said with certainty that a real difference exists.

It is obvious that metal-metal bonds are present in all of these compounds. It is of interest to investigate the predictions which can be made from Pauling's (15) equation

$$R(1) - R(n) = 0.30 \log n$$

This equation gives the difference in radius between bonds of bond numbers one and n. In this case n = v/12, where v is the number of electron pairs forming the twelve bonds in the Ta_6 (or Cb_6 or Mo_6) grouping. The single bond radii R(1) are given in Pauling's paper; they were calculated from the structures of

the pure metals using this same equation. If the assumption is made that the valence electrons of the chloride ions make no contributions to the metallic bonds, then $v = 3(5 - w)$ for columbium and tantalum, where w is the oxidation number. The oxidation numbers that correspond to the three suggested formulae are +3, +2 1/3, and +2. The predicted metallic radii are

Oxidation Number	Bond Number	Predicted Radius
+3	0.5	1.434 Å
+2 1/3	0.67	1.396 Å
+2	0.75	1.380 Å

for tantalum complexes; the corresponding radii for columbium are not significantly different. The experimentally determined radii are close enough to these values to be considered quite reasonable. If the equation is used to determine the bond numbers, the results are 0.41 for $Ta_6Br_{14}\cdot 7H_2O$, 0.47 for $Ta_6Cl_{14}\cdot 7H_2O$, and 0.53 for $Cb_6Cl_{14}\cdot 7H_2O$. It is not to be implied that these results favor one of the proposed oxidation states for tantalum and columbium. The equation is not considered sufficiently reliable for such a prediction. Moreover, the effect of the halogen atoms might well be far from negligible. The predicted molybdenum radius in the $(Mo_6Cl_8)^{++++}$ group is 1.30 Å if it is assumed that there are 3.78 valence electrons per molybdenum atom.

The shortest interatomic distances for chlorine and bromine in the tantalum and columbium complexes are somewhat shorter than twice the corresponding van der Waals' radii (1.80 for chlorine and 1.95 for bromine). This is not at all unusual,

however, since this is observed in a large number of cases where the halogens are in the same molecule and particularly where they are bound to the same atom.

It will be noticed that subtraction of the halogen radius from the corresponding metal-halogen distance gives a value for the metallic radius very nearly equal to one half the intermetallic distance. I do not mean to attach much significance to this observation other than that it indicates that these bonds are covalent and of reasonable magnitude. Subtracting the ionic halogen radii from the corresponding distances gives absurdly small values for the effective metallic radii. The covalent nature of these bonds is, of course, to be expected from the stability of the (Ta_6Cl_{12}) group.

REFERENCES

(1) Cyrill Brosset, Arkiv. för Kemi, Mineralogi och Geologi, A20 (1945).

(2) Cyrill Brosset, ibid. A22 (1946).

(3) K. Lindner, E. Haller, H. Helwig, A. Kohler, and H. Feit, Berichte, 55B, 1458 (1922).

(4) K. Lindner, E. Haller, and H. Helwig, Zeit. f. anorg. u. allgem chem., 130, 209 (1923).

(5) K. Lindner and H. Helwig, ibid. 142, 180-8 (1925).

(6) W. W. Scott, Standard Methods of Chemical Analysis, 4th Ed., Van Nostrand Co. p. 319.

(7) M. H. L. Pirenne, The Diffraction of X-Rays and Electrons by Free Molecules, Cambridge University Press, p. 79.

(8) E. E. Bray and N. S. Gingrich, J. Chem. Phys., 11, 351-4 (1943).

(9) A. Eisenstein, Phys. Rev., 63, 305-8 (1943).

(10) R. W. James, Physik. Zeit., 33, 737 (1932).

(11) P. A. Shaffer, V. Schomaker, and L. Pauling, J. Chem. Phys., 14, 659-64 (1946).

(12) F. J. Ewing and L. Pauling, Zeit. f. Krist., 68, 223-30 (1928).

(13) M. C. Chabrié, Compt. rend., 144, 804 (1907).

(14) W. H. Chapin, J. A. C. S., 32, 323 (1910).

(15) K. Lindner and H. Feit, Zeit. f. anorg. u. allgem. chem., 137, 66 (1924).

(16) O. R. Ruff and H. Thomas, Zeit. f. anorg. u. allgem. chem., 148, 1 and 19 (1925).

(17) H. S. Harned, J. A. C. S., 35, 1078 (1913).

(18) L. Pauling, J. A. C. S., 69, 542 (1947).

Propositions Submitted by Philip A. Vaughan

Ph.D. Oral Examination, May 9, 1949, 1:00 P.M., Crellin Conference Room.

Committee: Professors Sturdivant (Chairman), Pauling, Lucas, Schomaker, Davis; Drs. Hughes and Davidson.

1. The density of $CuCrO_2$ determined by Stroupe (1), 7.0 gm/cc, as well as his assignment of Z = 4, are probably incorrect. I suggest that Z = 3, corresponding to a density of 5.6 gm/cc. Steric considerations and his intensity data indicate the following probable structure:

Space group: D_{3d}^4 - $C6_22$
Basis: Cu in 1/2,0,0; 0,1/2,2/3; 1/2,1/2,1/3
Cr in 1/2,0,1/2; 0,1/2,1/6; 1/2,1/2,5/6
O in 1/2,0,z; 0,1/2,2/3 + z; 1/2,1/2,1/3 + z
1/2,0,z; 0,1/2,2/3 - z; 1/2,1/2,1/3 - z
with z ~ 1/4

The density of this compound should be redetermined.

(1) J. D. Stroupe, J.A.C.S. 71, 571 (1949).

2. Price and Zemany (1) have studied the equilibria

$$(CH_3)_2SiCl_2 + (CH_3)_4Si \longrightarrow 2(CH_3)_3SiCl \qquad (a)$$

and

$$(CH_3)SiCl_3 + (CH_3)_3SiCl \longrightarrow 2(CH_3)_2SiCl_2 \qquad (b)$$

and have determined the following thermodynamic data:

Reaction	$\Delta H^\circ_{385^\circ C}$, kcal/mol	ΔS, e.u.	$\Delta F^\circ_{385^\circ C}$, kcal/mol
(a)	-3.6	2.8	-5.4
(b)	-3.6	1.6	-4.7

I propose that the heat of reaction is due primarily to a heat of interaction of -1.8 kcal/mol between a chlorine atom and a methyl group. The heat of the reaction

$$(CH_3)_2SiCl_2 + SiCl_4 \longrightarrow 2CH_3SiCl_3$$

is predicted to be -3.6 kcal/mol. The heat content at 385°C of the methyl chlorosilanes can now be derived as functions of the heat content of $Si(CH_3)_4$ and $SiCl_4$.

(1) P. D. Zemany and F. P. Price, J.A.C.S., 70, 4222 (1948).

3. Pauling (1) has suggested an equation which relates bonded intermetallic distances to the bond order. I have applied this equation to liquid metals by assuming that there is a Gaussian distribution of bonded neighbors. The derived expression is

$$\overline{D} = D(1) + 0.26 \ln(N/v) + 0.366 w_{\frac{1}{2}}^2$$

where $\bar{D}$ is the mean bonded distance, w_i is the half width of the bonded neighbor distribution curve, and N is the average number of bonded neighbors. All of these quantities can be obtained by suitable measurements of the first peak of the radial distribution function for the metal. Using the radial distribution curves of C. Gamertsfelder (2), the following data were obtained:

Metal	Temp., °C	$\bar{D}_{calc}$, Å	$\bar{D}_{obs}$, Å
Tin	250	3.40	3.38
Indium	160	3.36	3.30
Zinc	460	3.00	2.94
Cadmium	350	3.15	3.06
Aluminum	700	2.99	2.96
Lithium	200	3.45	3.24

(1) L. Pauling, J.A.C.S., 69, 542 (1947).
(2) C. Gamertsfelder, J.C.P., 9, 450 (1941).

4. In order to increase the objectivity of the electron diffraction method for the determination of the structure of gas molecules, I suggest that final comparisons can be made with theoretical scattering photographs, which can be prepared by suitable optical methods.

5. (a) Brown (1) has measured the dissociation constants of the addition compounds of boron trimethyl with ammonia and the methylamines with what appears to be a high degree of precision. In such cases I suggest the use of the equation

$$\ln\left[\frac{K_p(T)}{(T/T_m)^4}\right] = \frac{1}{R}\left[-\frac{\Delta E_o^o}{T} - 4R + C_o + 4R \ln T_m\right]$$
$$= \frac{A}{T} + B \text{ (approximately)}$$

in deriving the thermodynamic functions. In this equation T_m is the mean temperature of the measurements and $S_{T_m} = C_o + 4R \ln T_m$. Brown's data on the addition compound of boron trimethyl with ammonia give:

$$\Delta S^o = (-6.58 \pm 0.20) + 4R \ln T$$
$$\Delta S^o_{347°K} = 39.9 \text{ cal/mol degree}$$
$$\Delta E^o_o = 11{,}000 \pm 70 \text{ cal/mol}$$
$$\Delta H^o_{347°K} = 13{,}760 \text{ cal/mol}$$

(b) Theoretical entropies and energies of the compounds involved in the above reaction were calculated; they are

Compound	$S^o_{347°K}$ e.u.	$E^o_{347°K}$ (vib. + int. rot.) cal/mol
$NH_3:B(CH_3)_3$	81.0	3800
NH_3	46.1	70
$B(CH_3)$	75.3	2940

This gives $\Delta S^{\circ}_{347^{\circ}K} = 40.4$ e.u. for the dissociation reaction. The method suggested by Rasmussen (2) to estimate the height of barriers to internal rotation and approximations similar to those suggested by Pitzer (3) to estimate vibrational entropies were used.

(1) H. C. Brown, H. Bartholomay, and M. D. Taylor, J.A.C.S., 66, 431 and 435 (1944).
(2) F. A. French and R. S. Rasmussen, J.C.P., 14, 389 (1946).
(3) K. S. Pitzer, J.C.P., 5, 473 (1937).

6. The following arguments can be presented against the concept of "B" strain as presented by Brown and coworkers (1):

(a) The heats of dissociation of the addition products of the methyl amines and ammonia with boron trimethyl can be readily accounted for if a heat of interaction of 3-4 kcal/mol per methyl-methyl interaction is assumed.
(b) His assumption of the essential absence of "F" strain in aqueous methyl-ammonium ions is not necessarily correct.
(c) His arguments concerning the relative ease of bond angle distortion before and after reaction with a proton are not convincing.

(1) H. C. Brown, H. Bartholomay, and M. D. Taylor, J.A.C.S., 66, 435 (1944).

7. Chromium sulfide which contains about 54 percent sulfur shows an interesting magnetic anomaly (1). At -180°C it is paramagnetic; the paramagnetic susceptibility increases with temperature up to about -120°C, at which temperature it becomes ferromagnetic. The ferromagnetic Curie point is about 20°C.

Chromium sulfide has the nickel arsenide (B-8) structure, in which the metal atoms are arranged in parallel, directly superposed, equilateral triangular nets. The spacing between the nets is somewhat smaller than the nearest neighbor distance within a net. The above magnetic behavior might occur if the exchange integral between nearest neighbors (J_1) is negative, and that between nearest neighbors within a net (J_2) is positive, and $|3J_2| > |J_1|$.

(1) H. Haraldsen, Zeit anorg. allgem. chem., 234, 337 (1937).

8. Although the structure of $Al_2(CH_3)_6$ suggested by Pitzer and Gutowsky (1) is the most logical one suggested thus far, the experimental evidence is certainly not unequivocal since (a) the vapor density measurements of Laubengayer and Gilliam (2) do not exclude the possibility of higher polymers, and (b) this structure gave only "fair" agreement with the electron diffraction data of Sutton and Skinner (3) while another dimer structure was listed as giving "good" agreement.

(1) K. S. Pitzer and H. S. Gutowsky, J.A.C.S., 68, 2204 (1946).
(2) A. W. Laubengayer and W. F. Gilliam, J.A.C.S., 63, 477 (1941).
(3) H. A. Skinner and L. E. Sutton, Nature, 156, 601 (1945).

9. (a) The explanation suggested by Bateman (1) for the shortening of the single bond in the 3 position in 1,5 diene systems such as is observed in geranylamine hydrochloride (2) does not appear plausible. Other similar dienes and di-ynes should be investigated in order to prove or disprove the generality of this anomaly.

(b) Welo's electrostatic explanation (3) for the large positive Weiss constant observed for polynuclear complexes such as $Cr_3(CH_3COO)_6(OH)_2\ Cl \cdot 8H_2O$ is probably incorrect. This effect might be caused by the close juxtaposition of cations in the complex.

(1) A. L. Bateman, Trans. Faraday Soc., 38, 367 (1942).
(2) G. A. Jeffrey, Proc. Roy. Soc., A183, 388 (1945).
(3) L. A. Welo, Phys. Rev., 32, 320 (1928).